

Style Definition: Comment Text

Convolutional Neural Network and Long Short-Term Memory Models for Ice-Jam ~~Prediction~~Predictions

Fatemehalsadat Madaeni¹, Karem Chokmani¹, Rachid Lhissou¹, Saied Homayouni¹, Yves Gauthier¹, and Simon Tolszczuk-Leclerc²

¹INRS-ETE, Université du Québec, Québec City, G1K 9A9, Canada

²EMGeo Operations, Natural Resources Canada, Ottawa, K1S 5K2, Canada

Correspondence to: Fatemehalsadat Madaeni (Fatemehalsadat.Madaeni@ete.inrs.ca)

Abstract. In cold regions, ice-jam events ~~jams frequently~~ result in severe flooding due to a rapid rise in water levels upstream of the jam. ~~These~~Sudden floods resulting from ice jams threaten human safety, and cause damage to properties and ~~infrastructures as the floods resulting from ice jams are sudden~~infrastructure. Hence, ice-jam prediction tools can give an early warning to increase response time and minimize the possible ~~corresponding~~ damages. However, ice-jam prediction has always been a ~~challenging problem~~challenge as there is no analytical method available for this purpose. Nonetheless, ice jams form when some hydro-meteorological conditions happen, a few hours to a few days before the event. Ice-jam prediction ~~problem~~ can be ~~considered~~addressed as a binary multivariate time-series classification. Deep learning techniques have been widely used for time-series classification in many fields such as finance, engineering, weather forecasting, and medicine. In this research, we successfully applied ~~Convolutional Neural Network~~convolutional neural networks (CNN), ~~Long Short-Term Memory~~long short-term memory (LSTM), and combined ~~Convolutional Long Short-Term Memory~~convolutional-long short-term memory (CNN-LSTM) networks ~~for to predict the formation of ice-jam prediction for jams in~~ 150 rivers in the Province of Quebec (Canada). We also employed machine learning methods including support vector machine (SVM), k-nearest neighbors classifier (KNN), decision tree, and multilayer perceptron (MLP) for this purpose. The hydro-meteorological variables (e.g., temperature, precipitation, and snow depth) along with the corresponding jam or no-jam events are used as ~~the model~~ inputs ~~to the models. We hold out 10%. Ten percent~~ of the data ~~was excluded from the model and set aside~~ for testing. ~~And we applied, and~~ 100 ~~re-shuffling~~reshuffling and splitting iterations ~~with were applied to~~ 80% of the remaining data for training and 20% for validation. The developed deep learning models achieved improvements in performance in comparison to the developed machine learning models. The results show that the CNN-LSTM model yields the best results in the validation and testing with F1 scores of 0.82 and 0.92, respectively. This demonstrates that CNN and LSTM models are complementary, and a combination of ~~them both~~ further improves classification.

Formatted: English (United Kingdom)

1 Introduction

Predicting ice-jam events ~~jams~~ gives an early warning of possible flooding events, but there is no analytical solution to predict these events due to the complex interactions between ~~involved the~~ hydro-meteorological variables (e.g., temperature, precipitation, snow depth, and solar radiation). ~~involved~~. To date, a small number of empirical and statistical prediction methods such as threshold methods, multi-regression models, logistic regression models, and discriminant function analysis have been developed for ice jams (Barnes-Svarney and Montz, 1985; Mahabir et al., 2006; Massie et al., 2002; White, 2003; White and Daly, 2002, ~~January~~; Zhao et al., 2012). However, these methods

38 are site-specific ~~with and have~~ high ~~rates~~ of false-positive errors (White, 2003). The numerical models developed
39 for ice-jam prediction (e.g., ICEJAM (Flato and Gerard, 1986, cf.; Carson et al., 2011), RIVJAM (Beltaos, 1993),
40 HEC-RAS (Brunner, 2002), ICESIM (Carson et al., 2001 and 2003), and RIVICE (Lindenschmidt, 2017)) ~~show~~
41 ~~several~~ limitations in predicting ice-jam occurrence. ~~This is because. More particularly, the~~ mathematical formulations
42 ~~used~~ in these models are complex ~~which and~~ need many parameters ~~that, which~~ are often unavailable as they are
43 challenging to measure in ice conditions. ~~Hence, many~~The subsequent simplifications ~~corresponding~~necessary to these
44 ~~parameters may degrade~~model application decrease model accuracy (Shouyu & Honglan, 2005). A detailed overview
45 of the previous models for ice-jam prediction based on hydro-meteorological data ~~are~~is presented in Madaeni et al.
46 (2020).

47 Prediction of ice-jam occurrence can be considered as a binary multivariate time-series classification (TSC) problem
48 when the time series of various ~~hydro-meteorological~~hydro-meteorological variables ~~(explained later)~~ can be used to
49 classify jam or no jam events. Time-series classification (particularly multivariate) has been widely used in various
50 fields, including biomedical engineering, clinical prediction, human activity recognition, weather forecasting, and
51 finance. Multivariate time-series provide more patterns and improve classification performance compared to
52 univariate time-series (Zheng et al., 2016). Time-series classification is one of the most challenging problems in data
53 mining and machine learning.

54 Most existing TSC methods are feature-based, distance-based, or ensemble methods (Cui et al., 2016). Feature
55 extraction is challenging due to the difficulty of handcrafting useful features to capture intrinsic characteristics from
56 time-series data (Karim et al., ~~2019~~2019a; Zheng et al., 2014, ~~June~~). Hence, distance-based methods work better in
57 TSC (Zheng et al., 2014, ~~June~~). Among the hundreds of methods developed for TSC, the leading classifier with the
58 best performance was ~~an~~ ensemble nearest neighbor ~~approach~~ with dynamic time warping (DTW) ~~for many years~~
59 (Fawaz et al., ~~2019, July~~2019a; Karim et al., ~~2019~~2019a).

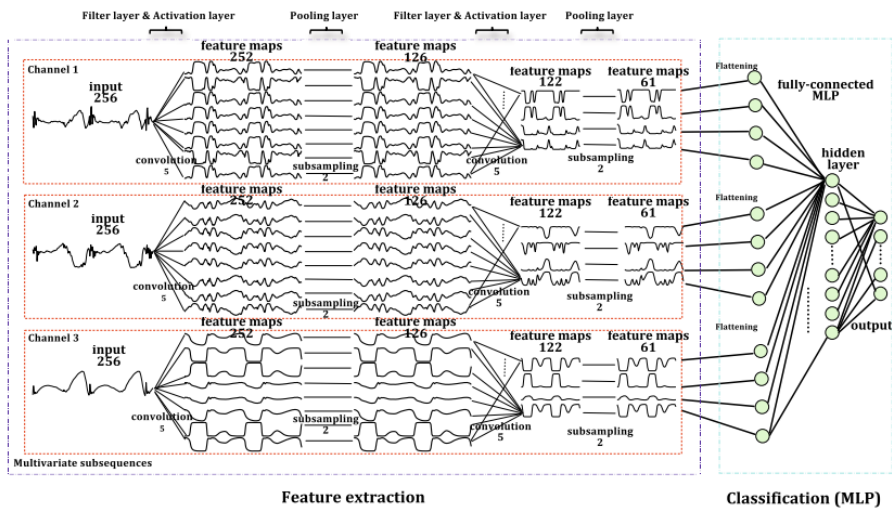
60 In the k-nearest neighbors (KNN) classifier, the ~~given~~-test instance is classified by ~~at the~~ majority vote of its k-~~closest~~-
61 ~~nearest~~ neighbors in the training ~~data~~dataset. The ~~KNN classifier needs all the data~~entire dataset is necessary to make
62 a prediction ~~based of~~ KNN, which requires ~~high a~~ lot of processing memory. Hence, it is computationally expensive
63 and ~~could be slow if~~time-consuming when the database is large, ~~and, It is also~~ sensitive to irrelevant features and
64 ~~the data~~ scale of the data. Furthermore, the number of neighbors ~~to include~~included in the algorithm should be carefully
65 selected. The KNN classifier is very challenging to be used for multivariate TSC. The dynamic time warping ~~approach~~
66 is ~~a more~~ robust alternative for Euclidean distance (the most widely used time-series distance measure) to measure the
67 similarity between two ~~given~~-time series by searching for an optimal alignment (minimum distance) between them
68 (Zheng et al., 2016). However, the combined KNN with DTW is time-consuming and inefficient for long multivariate
69 time-series (Lin et al., 2012; Zheng et al., 2014, ~~June~~). ~~The traditional~~, ~~Traditional~~ classification and ~~classic~~ data
70 mining algorithms developed for TSC have high computational complexity or low prediction accuracy. This is due to
71 the size and inherent complexity of time series, seasonality, noise, and feature correlation (Lin et al., 2012).

72 There are some machine learning methods available for TSC such as KNN and support vector machine (SVM).
73 However, the focus of this research is on the deep learning models that have greatly ~~impacted~~improved sequence
74 classification ~~problems and they can also be used for that perform well with~~ multivariate TSC ~~with good performance.~~

75 Deep learning methods ~~are able to consider two dimensionality in~~ work with 2-D multivariate time-series and their
76 deeper architecture could further improve ~~the~~ classification especially for complex problems, ~~which is~~. This explains
77 why ~~their results are~~ deep learning methods generally have more accurate and robust results than other currently used
78 methods (Wu et al., 2018a, April 2018). However, ~~they are~~ their training is more time consuming and ~~their~~
79 ~~interpretation is more~~ difficult to interpret.

80 Deep learning is a type of ~~involves~~ neural networks that ~~uses~~ use multiple layers where nonlinear transformation is used
81 to extract
82 higher-level features from the input data. Although deep learning ~~in recent years showed~~ has recently shown promising
83 performance in various fields such as image and speech recognition, document classification, and natural language
84 processing, only a few studies ~~employed~~ were dedicated to using deep learning for TSC (Gu et al., 2018; Fawaz et al.,
85 2019, July 2019a). Various studies show that deep neural networks significantly outperform the ensemble nearest
86 neighbor with DTW (Fawaz et al., 2019, July 2019a). The main benefit of deep learning networks is automatic feature-
87 extraction, which reduces the need for expert knowledge ~~of the field~~ and removes engineering bias ~~in the~~ during
88 classification ~~task~~ (Fawaz et al., 2019) as the probabilistic decision (e.g., classification) is taken by the network-
89 (Fawaz et al., 2019b).

90 The most widely used deep neural networks for TSC are ~~Multi-Layer Perceptron~~ multi-layer perceptron (MLP; i.e.,
91 fully connected deep neural networks), ~~Convolutional Neural Networks~~ convolutional neural networks (CNNs), and
92 ~~Long Short-Term Memory~~ long short-term memory networks (LSTM). The application of CNNs for TSC has recently
93 become ~~more and more~~ increasingly popular, and different types of CNN are being developed with superior accuracy
94 for this purpose (e.g., Cui et al., 2016). Zheng et al. (2014, June) and Zheng et al. (2016) introduce a ~~Multi-Channels~~
95 ~~Deep Convolutional Neural Network~~ multi-channel deep convolutional neural network (MC-DCNN) for multivariate
96 TSC, where each variable (i.e., univariate time series) is trained individually to extract features and finally
97 concatenated using an MLP to perform classification (Fig. 1). ~~They~~ The authors showed that their model achieves a
98 state-of-the-art performance ~~both in~~ terms of efficiency and accuracy on a challenging dataset. The drawback of their
99 model and similar architectures (e.g., Devineau et al., 2018, May 2018a) is that they do not capture the correlation
100 between variables as the feature extraction is carried out separately for each variable.



101

102 **Figure-1. A 2-stage MC-DCNN architecture for activity classification. This architecture consists of a three**
 103 **channels-channel input, two filter layers, two pooling layers, and two fully-connected layers (after Zheng et al., 2014, June).**

104 Brunel et al. (2019) present CNNs adapted for TSC in cosmology using \mathbb{H}^1 -D filters to extract features from each
 105 channel over time and a \mathbb{H}^1 convolution in depth to capture the correlation between the channels. They compared the
 106 results from LSTMs with those from CNNs, which shows and demonstrated that CNNs give had better results than
 107 LSTMs. Nevertheless, both deep learning approaches are very promising.

108 The combination of CNNs and LSTM units has already yielded state-of-the-art promising results in problems requiring
 109 classification of temporal information classification, such as human activity recognition (Li et al., 2017; Mutegeki and
 110 Han, 2020, February), text classification (Luan and Lin, 2019; March, She and Zhang, 2018, December; Umer et
 111 al., 2020), video classification (-Lu et al., 2018 and Wu et al., 2015, October), sentiment analysis (Ombabi et al., 2020;
 112 Sosa, 2017; Wang et al., 2016, August; Wang et al., 2019),- typhoon formation forecasting (Chen et al., 2019), and
 113 arrhythmia diagnosis (Oh et al., 2018). In this architecture, convolutional operations capture features and LSTMs
 114 capture time dependencies on the extracted features. Ordóñez and Roggen (2016) propose a deep convolutional LSTM
 115 model (DeepConvLSTM) for activity recognition (Fig. 2). Their results are compared to the results from standard
 116 feedforward units showing that DeepConvLSTM reaches a higher F1 score and better decision boundaries for
 117 classification. Furthermore, they noticed that the LSTM model gives is also promising results with relatively small
 118 datasets. Furthermore, LSTMs present a perform better performance in capturing with longer temporal dynamics,
 119 whereas the convolution filters can only capture the temporal dependencies dynamics within the length of the filter.

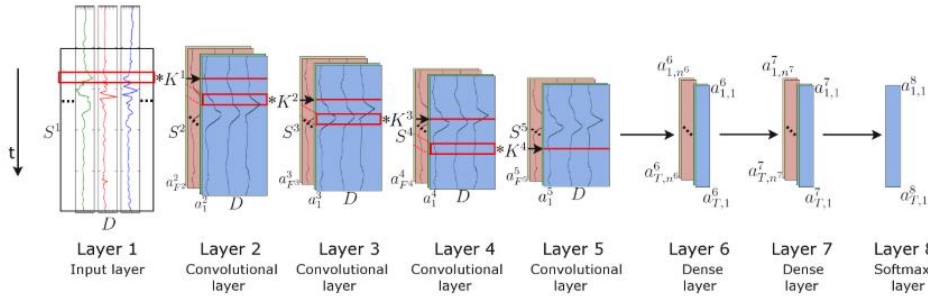


Figure 2. The architecture of the DeepConvLSTM framework used for activity recognition (after Ordóñez and Roggen, 2016).

This project presented in this paper is a part of a greater project called DAVE, which aims to develop a tool to provide regional ice jam watches and warnings, based on the integration of three aspects: the current ice cover conditions of the ice cover; hydro-meteorological patterns associated with breakup ice jams; and channel predisposition to ice-jam formation. The outputs of the previous tasks will be used to develop an ice-jam monitoring and warning module and that will transfer the knowledge gained to the end-users to better manage the risk of managing ice jam consequences.

The objective of this research is to develop deep learning models to predict breakup ice-jam events to be used as an early warning system of possible flooding. While most TSC research in deep learning is performed on 1-D channels (Hatami et al., 2018, April, we propose), our approach consists of using deep learning frameworks for multivariate TSC for applied to ice-jam prediction. Through our comprehensive literature review, we noticed that CNN (e.g., Brunel et al., 2019; Cui et al., 2016; Devineau et al., 2018, June 2018b; Kashiparekh, 2019, July; Nosratabadi et al., 2020; Yan et al., 2020; Yang et al., 2015, June; Yi et al., 2017; Zheng et al., 2016), LSTM (e.g., Fischer and Krauss, 2018; Lipton et al., 2015; Nosratabadi et al., 2020; Torres et al., 2021), and a combined CNN-LSTM (e.g., Karim et al., 2017, 2017; Livieris et al., 2020; Ordóñez and Roggen, 2016; Sainath et al., 2015, April; Xingjian et al., 2015) have been widely used for TSC. There are numerous applications of CNN, LSTM, and their hybrid versions applied are currently used in the field of hydrology (Althoff et al., 2021; Apaydin et al., 2020; Barzegar et al., 2021, 2020; Kratzert et al., 2018; Wunsch et al., 2020; Zhang et al., 2018). Although deep learning methods seem to be promising to address the requirements of ice-jam predictions, none of these methods yet have been explored for ice-jam prediction.

Hence, although machine learning methods have been widely used in time series forecasting of hydro-meteorological data, they have been used less frequently in the prediction of ice jams (Graf et al., 2022). Semenova et al. (2020) used KNN to predict ice jams using hydro-meteorological variables such as precipitation, snow depth, water level, water discharge, and temperature. They developed their model with data collected from the confluence of Sukhona River and Yug River in Russia between 1960 and 2016 and achieved accuracy of 82%. Sarafanov et al. (2021) presented an ensemble-based model of machine learning methods and a physical snowmelt-runoff model to account for the advantages of physical models (interpretability) and machine learning models (low forecasting error).

149 ~~Their hybrid models proposed an automated approach for short-term flood forecasting in Lena River, Poland, using~~
150 ~~hydro-meteorological variables (e.g., maximum water level, mean daily water and air temperature, mean daily water~~
151 ~~discharge, relative humidity, snow depth, and ice thickness). They applied an automated machine learning approach~~
152 ~~based on the evolutionary algorithm to automatically identify machine learning models, tune hyperparameters, and~~
153 ~~combine stand-alone models into ensembles. Their model was validated on ten hydro gauges for two years, showing~~
154 ~~that the hybrid model is much more efficient than stand-alone models with a Nash–Sutcliffe efficiency coefficient of~~
155 ~~0.8. Graf et al. (2022) developed an MLP and extreme gradient boosting model to predict ice jams with data from~~
156 ~~1983 to 2013, in Warta River, Poland. They employed water and air temperatures, river flow, and water level as inputs~~
157 ~~to their models, showing that both machine learning methods provide promising results. In Canada, De Coste et al.~~
158 ~~(2021) developed a hybrid model including a number of machine learning models (e.g., KNN, SVM, random forest,~~
159 ~~and gradient boosting) for St. John River (New Brunswick). The most successful ensemble model combining 6~~
160 ~~different member models was produced with a prediction accuracy of 86% over 11 years of record.~~
161 ~~We developed three deep learning models; a CNN, an LSTM, and a combined CNN-LSTM for ice-jam predictions,~~
162 ~~and compared the results. The previous studies show that these models ~~show good capabilities in capturing~~successfully~~
163 ~~capture~~ features ~~and~~, the correlation between features (through convolution units) and time dependencies (through
164 memory units) ~~that will be later~~which are subsequently used for TSC. The combined CNN-LSTM can reduce errors
165 by compensating for the internal weaknesses of each model. In the CNN-LSTM model, CNNs capture features, then
166 the LSTMs ~~give the~~identifies time dependencies on the captured features.
167 Furthermore, we also developed some machine learning methods as simpler methods for ice-jam prediction. And their
168 results are compared with ~~results~~those obtained from the ~~developed~~ deep learning models.

169 2 Materials and Methods

170 2.1 Data and study area

171 It is known that specific hydro-meteorological conditions lead to ice-jam occurrence (Turcotte and Morse, 2015,
172 ~~August~~; and White, 2003). For instance, breakup ice jams occur when a period of intense cold is followed by a rapid
173 peak discharge resulting from spring rainfall and snowmelt runoff (Massie et al., 2002). ~~The period of intense cold~~
174 ~~can be represented by the changes in~~Accumulated Freezing Degree Days/freezing degree days (AFDD). ~~The sudden~~
175 ~~can be used as a proxy for intense cold periods. Sudden~~ spring runoff increase, ~~however~~, is not often available at the
176 jam location and can be represented by liquid precipitation and snow depth ~~somea few~~ days ~~before~~prior to ice-jam
177 occurrence (Zhao et al., 2012). Prowse and Bonsal (2004) and Prowse et al. (2007) ~~evaluate~~assessed various
178 hydroclimatic explanations for river ice freeze-up and breakup, concluding that shortwave radiation is the most critical
179 factor influencing the mechanical strength of ice and consequently the possibility of breakup ice jams to occur.
180 Turcotte and Morse (2015, ~~August~~) explain that ~~Accumulated Thawing Degree Day~~accumulated thawing degree day
181 (ATDD), an indicator of warming periods, partially covers the effect of shortwave radiation. ~~In the~~ previous studies
182 ~~of~~addressing ice-jam and breakup predictions, discharge and changes in discharge, water level and changes in water
183 level, AFDD, ATDD, precipitation, solar radiation, heat budget, and snowmelt or snowpack are the most
184 ~~readily~~frequently used variables (Madaeni et al., 2020).

185 The inputs we used in this study are historical ice-jam or no ice-jam occurrence (Fig. 3) as well as hydro-
 186 meteorological variables including from 150 rivers in Quebec, namely liquid precipitation (mm), minimum and
 187 maximum temperature (°C), AFDD (from August 1st of each year; °C), ATDD (from January 1st of each year;
 188 °C), snow depth (cm) and net radiation ($W\ m^{-2}$) in 150 rivers in Quebec. The net solar radiation, which represents
 189 the total energy available to influence the climate, is calculated as the difference between incoming and outgoing
 190 energy. If the median temperature is greater than 1, the precipitation is considered to be liquid precipitation. The
 191 statistics of hydro-meteorological data used in the models are presented in Table 1. The source, time period, and
 192 spatial resolution of the input variables are shown in Table 2.

193 **Table 1. Statistics of hydro-meteorological variables used in the models.**

Statistic	Liquid Precipitation (mm)	Minimum temperature (°C)	Maximum temperature (°C)	Net radiation ($W\ m^{-2}$)	ATDD (°C)	AFDD (°C)	Snowdepth (cm)
Minimum	0.00	-40.00	-25.97	-67.77	0.00	2109.33	0.00
Maximum	50.87	12.05	27.48	222.69	280.82	-35.41	121.86
Mean	1.04	-9.41	0.98	59.75	8.83	-898.48	15.99
Median	0.00	-7.73	1.68	59.41	1.27	-890.74	11.50

Formatted: Normal, Justified, Line spacing: 1.5 lines, Don't keep with next, Pattern: Clear (White)

Formatted: Font: 9 pt, Bold, Font color: Text 1, English (United States)

194

195

196 **Table 2. Source, duration, and spatial resolution of hydro-meteorological data used in the models.**

Data	Source	Duration	Spatial resolution
Min and Max temperature*	Daily Surface Weather Data (Daymet; Thornton et al., 2020)	1979–2019	1 km
Liquid precipitation	Canadian Precipitation Analysis (CaPA; Mahfouf et al., 2007)	2002–2019	10–15 km
Liquid precipitation	North American Regional Reanalysis (NARR; Mesinger et al., 2006)	1979–2001	30 km
Infrared radiation emitted by the atmosphere	North American Regional Reanalysis (NARR)	1979–2019	30 km
Infrared radiation emitted from the surface	North American Regional Reanalysis (NARR)	1979–2019	30 km
Snow depth	North American Regional Reanalysis (NARR)	1979–2019	30 km

Formatted: Font: 10 pt, English (Canada)

Formatted: Justified, Line spacing: 1.5 lines, Pattern: Clear (White)

197 * The average was used to derive the AFDD and the ATDD.

198

199 Ice-jam database is/was provided by the Quebec Ministry of Public Security (provincial public safety department
 200 (Ministère de la sécurité publique du Québec; MSPQ; Données Québec, 2021) for 150 rivers in Quebec, mainly in the
 201 St. Lawrence basin/River Basin. The database comes from the digital or paper event report/events reported by local
 202 authorities under the jurisdiction of the MSPQ from 1985 to 2014. Moreover, some other data refused to build this
 203 database were provided by the field observations from/collected by the Vigilance/Flood application from 2013 to
 204 2019. It contains 995 recorded jam events that are not validated and contain many inaccuracies, mainly in the
 205 toponymy of the rivers, location, dating, and the jam event redundancy of jam events.

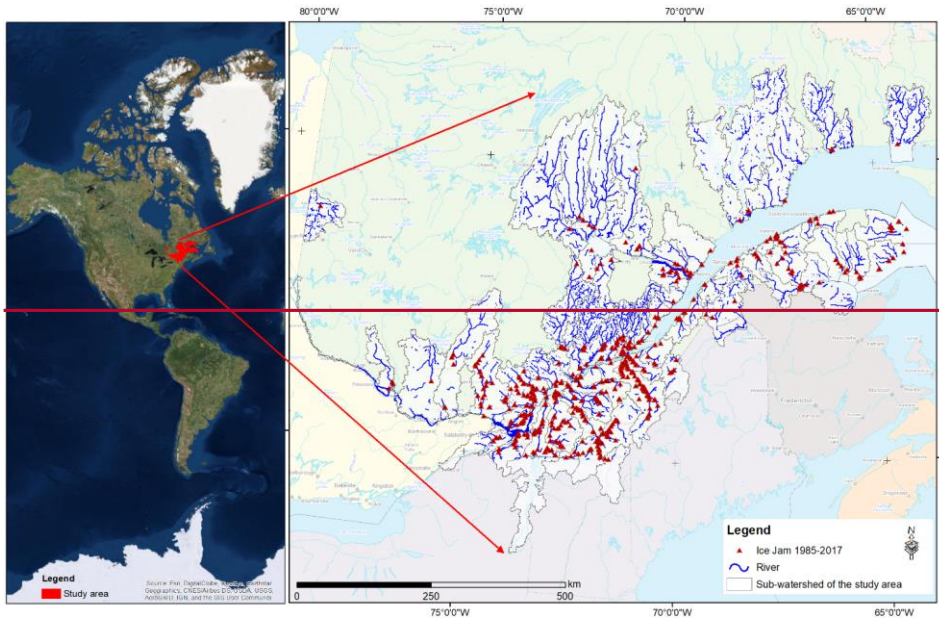
206 The names of the watercourse of several recorded jams are not given or completely wrong or affected by a typo or an
 207 abbreviation misspelled. The toponymy of the rivers was corrected using the National Hydrographic Network (NHN;
 208 National Hydrographic Network - Natural Resources Canada (NRCan)), the Geobase/GeoBase of the Quebec
 209 hydrographie network/Hydrographic Network (National Hydro Network - NHN - GeoBase Series - Natural Resources

210 Canada), and the Toporama Web map service (The Atlas of Canada - Toporama - Natural Resources Canada) of the
211 Sector of Earth Sciences.

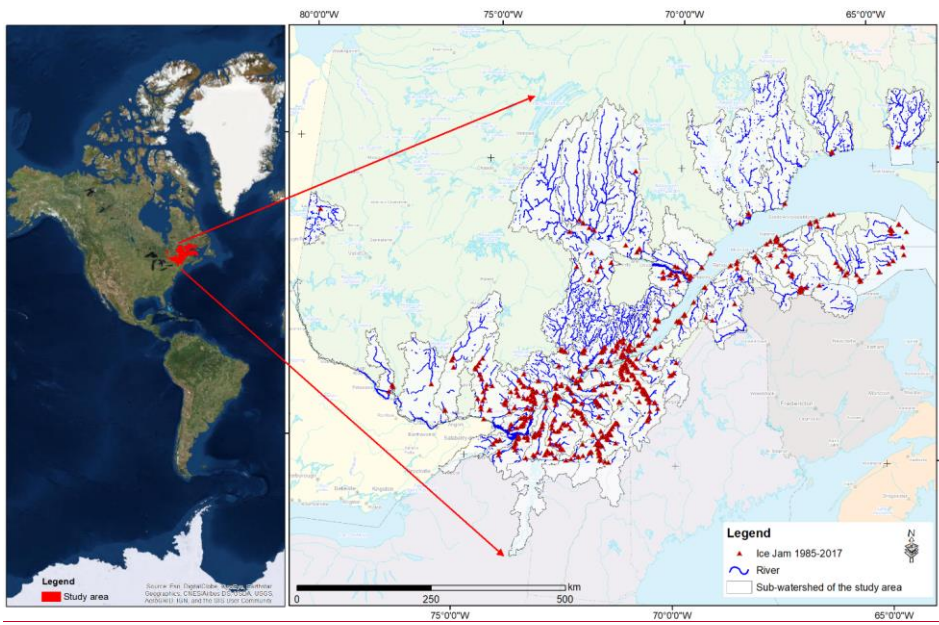
212 ~~Several~~Other manual corrections had to be carried out on ice jam data. For example, ice jams ~~are~~location is sometimes
213 placed on the ~~banks~~riverbanks at a small distance (less than 20_m) from the ~~river~~ polygon ~~of the river~~. In this case,
214 the location of the ice jam is manually moved inside the river polygon. In other cases, the ice-jam point is ~~posed~~placed
215 further on the flooded shore at a distance between 20_m and 200-~~m~~. m from the true ice jam. This ~~has been~~was
216 corrected based on images with very high spatial resolution, based on the sinuosity and the narrowing of the river, the
217 history of ice jams at the site ~~in question~~, and ~~the~~ press archives. In addition, some ice jams were placed too far from
218 the ~~mentioned~~ river due to wrong ~~recorded~~ coordinates in the database. A single-digit correction in longitude or
219 latitude returned the jam to its exact location. There are certain cases where the date of jam formation is verified by
220 searching ~~the~~ press archives, notably when the date of formation is missing or several jams with the same dates and
221 close locations in a section of a river are present.

222 The ice jam database contains many duplicates. This redundancy can be ~~due to~~explained by the merging of two ~~data~~
223 ~~sources, the databases, a~~ double entry during ice_jam monitoring, or ~~recording numerous recordings for~~ an ice jam
224 ~~that lasted~~ for several days. ~~The~~To remediate this, ~~the~~ duplicates ~~are~~were removed from the database. The corrected
225 ice-jam database contains 850 jams for 150 rivers, mainly in southern Quebec (Fig. 3). ~~The ice~~Ice jams formed in
226 November and December (freeze-up jams) are removed ~~to only include~~from the model since the processes involved
227 ~~are different from~~ breakup ice jams (included from January ~~15th~~) in the modelling as these two types of jams are
228 ~~formed due to different processes~~.¹⁵). The final breakup ice-jam database ~~that~~ used in this study includes 504 jam
229 events.

230



231



232

Figure 3. Study area and historic ice-jam locations recorded in Quebec from 1985- to 2017.

233 **Table 1. Statistics of hydro-meteorological variables used in the models.**

Statistics	Liquid P (mm)	Tmin (°C)	Tmax (°C)	Net-radiation (W-m-2)	ATDD (°C)	AFDD (°C)	Snowdepth (cm)
min	0.00	-40.00	-25.97	-67.77	0.00	-2109.33	0.00
max	50.87	12.05	27.48	222.60	280.82	-35.41	121.86
average	1.04	-9.41	0.98	59.75	8.83	-898.48	15.99
median	0.00	-7.73	1.68	59.41	1.27	-890.74	11.50

Formatted: Font: 9 pt, Bold, Font color: Text 1, English (United States)

Formatted: Normal, Justified, Line spacing: 1.5 lines, Don't keep with next, Pattern: Clear (White)

234
235 **Table 2. Source, duration, and spatial resolution of hydro-meteorological data used in the models.**

Data	Source	Duration	Spatial resolution
Min and Max temperature*	Daily Surface Weather Data (Daymet; Thornton et al., 2020)	1979-2019	1 km
Liquid precipitation	Canadian Precipitation Analysis (CaPA; Mahfouf et al., 2007)	2002-2019	10-15km
Liquid precipitation	North American Regional Reanalysis (NARR; Mesinger et al., 2006)	1979-2001	30 km
Infrared radiation emitted by the atmosphere	North American Regional Reanalysis (NARR)	1979-2019	30 km
Infrared radiation emitted from the surface	North American Regional Reanalysis (NARR)	1979-2019	30 km
Snow depth	North American Regional Reanalysis (NARR)	1979-2019	30 km

236 *The average was used to derive the AFDD and the ATDD.

Formatted: Font: 10 pt, English (Canada)

Formatted: Justified, Line spacing: 1.5 lines, Pattern: Clear (White)

237
238 **2.2 Machine learning models for TSC**

239 The most common machine learning techniques that have been used for TSC are SVM (Rodríguez and Alonso, 2004; Xing and Keogh, 2010), KNN (Li et al., 2013; Xing and Keogh, 2010), decision tree (DT; Brunello et al., 2019; Jović et al., 2012, August), and multilayer perceptron (MLP; del Campo et al., 2021; Nanopoulos et al., 2001). For more information about these machine learning models refer to the mentioned literature above. We do not explain these These models and their applications in TSC, as they are not beyond the focus scope of this study and will not be further addressed.

Formatted: Caption, Pattern: Clear

Formatted: Font color: Text 1

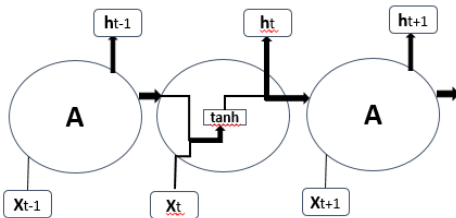
Formatted: Normal, Left, Space Before: 0 pt, After: 0 pt, Pattern: Clear (White)

245 We developed the mentioned machine learning methods and compared their results with the results those of deep learning models. After some trials and errors, the parameters that are changed from the default values for each machine learning model are as follows. We developed an SVM with a polynomial kernel with a degree of 5 that can distinguish curved or nonlinear input space. The KNN is used with 3 neighbors used for classification. The decision tree model is applied with all the default values. The shallow MLP is used with "lbfgs" solver (which can converge faster and perform better for small datasets), alpha of 1e-5, and 3 layers with 7 neurons in each layer.

251 **2.3 Deep learning models for TSC**

252 The most common and popular deep neural networks for TSC are MLPs, CNNs, and LSTMs (Brownlee, 2018; and Torres et al., 2021). Despite their power, however, Although it is very powerful approach, MLP has limitations networks are limited by the fact that each input (i.e., time-series element) and output are treated independently, which means that the temporal or space information is lost (Lipton et al., 2015). Hence, an MLP needs some temporal information in the input data to model sequential data, such as time series (Ordóñez and Roggen, 2016).

257 In this regard, ~~Recurrent Neural Networks~~ recurrent neural networks (RNNs) are specifically adapted to sequence data
 258 through the direct connections between individual layers (Jozefowicz et al., 2015). Recurrent ~~Neural Networks~~ neural
 259 ~~networks~~ perform the same repeating function with a straightforward structure, e.g., a single tanh (hyperbolic tangent)
 260 layer, for every input of data (x_t), ~~while all~~ the inputs are related to each other ~~with~~ within their hidden internal
 261 state, which allows it to learn the temporal dynamics of sequential data (Fig. 4).



262
 263 **Figure 4. An RNN with a single tanh layer, where A is a chunk of the neural network, x is input data, and h is output data.**

264 Recurrent ~~Neural Networks~~ ~~were~~ ~~neural networks~~ are rarely used in TSC due to their significant ~~problems~~. ~~Recurrent~~
 265 ~~Neural Networks~~ ~~mainly~~ ~~limitations~~: ~~RNNs~~ ~~mostly~~ predict ~~output~~ ~~outputs~~ for each time-series element; they are
 266 sensitive to the first examples seen, and it is ~~also~~ challenging to capture long-term dependencies due to vanishing
 267 gradients, exploding gradients, and their complex dynamics (Devineau et al., ~~2018~~, ~~June~~ ~~2018~~ ~~b~~; Fawaz et al.,
 268 ~~2019~~ ~~2019~~ ~~b~~).

269 Long short-term memory RNNs are developed to improve the performance of RNNs by integrating a memory
 270 ~~component~~ to model long-term dependencies in time-series problems (Brunel et al., 2019; Karim et al., ~~2019~~ ~~2019~~ ~~a~~).

271 Long short-term memory networks do not have the problem of exploding gradients. The LSTMs have four interacting
 272 neural network layers in a very special way (Fig. 5). An LSTM has three sigmoid (σ) layers to control how much of
 273 each component should be let through by outputting numbers between zero and one. The input to an LSTM goes
 274 through three gates (“forget”, “input”, and “output gates”) that control the operation performed on each LSTM block
 275 (Ordóñez and Roggen, 2016). The first step is the “forget gate” layer that gets the output of the previous block (h_{t-1}),
 276 the input for the current block (x_t), and the memory of the previous block (C_{t-1}) and gives a number
 277 between 0 and 1 for each number in the cell state (C_t ; Olah, 2015). The second step is called the “input gate” with
 278 two parts, a sigmoid layer that decides which values to be updated and a tanh layer that creates new candidate values
 279 for the cell state. ~~These two~~ ~~The~~ new and old memories ~~will~~ ~~are~~ then be combined and control how much the new
 280 memory should influence the old memory. The last step (output gate) gives the output by applying a sigmoid layer
 281 deciding how much new cell memory goes to output, and ~~multiply~~ ~~multiplies~~ it by tanh applied to the cell state
 282 (~~giving~~ ~~resulting in~~ values between -1 and 1).

Formatted: Font: Italic
 Formatted: Font: Italic
 Formatted: Font: Italic

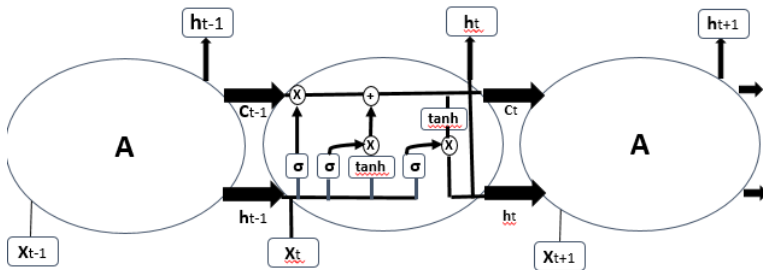


Figure_5. Structure of LSTM block with four interacting layers.

Recently, convolutional neural networks challenged the assumption that RNNs (e.g., LSTMs) have the best performance when working with sequences. The CNNs show state-of-the-art performance in Convolutional NNs perform well when processing sequential data such as speech recognition and sentence classification, similar to TSC (Fawaz et al., 2019, 2019b).

The CNNs Convolutional NNs are the most widely used deep learning methods in TSC problems (Fawaz et al., 2019, 2019b). They learn spatial features from raw input time series using filters (Fawaz et al., 2019, 2019b). Convolutional NNs are robust and need a relatively small amount of training time comparing with compared to RNNs or MLPs. They work best for extracting local information and reducing the complexity of the model.

A CNN is a kind of neural network with at least one convolutional (or filter) layer. A CNN usually involves several convolutional layers, activation functions, and pooling layers for feature extraction following, followed by dense layers (or MLP) used as a classifier classifiers (Devineau et al., 2018, June 2018b). The reason to use a sequence of filters is to learn various features from time series for TSC. A convolutional layer consists of a set of learnable filters that compute dot products between local regions in the input and corresponding weights. With high-dimensional inputs, it is impractical to connect subsequent neurons to all the neurons in of the previous layer. Therefore, each neuron in CNNs is connected to only a local region of the input, namely the receptive field, which equals whose size is equivalent to that of the filter size (Fig. 6). This feature reduces the number of parameters by limiting the number of connections between neurons in different layers. The input is first convolved with a learned filter, and then an element-wise nonlinear activation function is applied to the convolved results (Gu et al., 2018). The pooling layer performs a downsampling operation such as maximum or average, reducing the spatial dimension. One of the most powerful features of CNNs is called weight or parameter sharing, where all neurons share filters (weights) in a particular feature map (Fawaz et al., 2019, 2019b). This allows to reduce the number of parameters.



Figure-6. A Structure of a convolution layer structure including two sets of filters.

Formatted: Font: 9 pt

2.4 Model libraries

In an Anaconda (Analytics, C., 2016) environment, Python is implemented to develop CNN, LSTM, and CNN-LSTM networks for TSC. To build and train networks, the networks are implemented in Theano (Bergstra et al., 2010, June) using the Lasagne library (Dieleman et al., 2015) library. The other core libraries used for importing, preprocessing, training data, and visualization of results are include Pandas (Reback et al., 2020), NumPy (Harris et al., 2020), Scikit-Learn (Pedregosa et al., 2011), and Matplotlib_PyLab (Hunter, J.-D., 2007). The Spyder (Raybaut, 2009) package of Anaconda is utilized can be used as an interface, or otherwise, the command window can be used without any interface.

To develop machine learning models, Scikit-Learn machine learning libraries are used except for NumPy, Pandas, and Scikit-Learn preprocessing libraries.

2.5 Preprocessing

The data is comprised of variables with varying scales, and the machine-learning algorithms can benefit from rescaling the variables to all have the same single scale. Scikit-learn (Pedregosa et al., 2011) is a free library for machine learning in Python that can be used to preprocess data. We examined Scikit-learn MinMaxScaler (scaling each variable between 0 and 1), Normalizer (scaling individual samples to the unit norm), and StandardScaler (transforming to zero mean and unit variance separately for each feature). The results show that MinMaxScaler (Eq. (1)) leads to the most accurate results. The scaling of validation data rescaling is done with min carried out based on minimum and max from maximum values of the train data.

$$X_{\text{scaled}} = \frac{X - X_{\text{min}}}{X_{\text{max}} - X_{\text{min}}} \frac{X_{\text{max}} - X_{\text{min}}}{X_{\text{max}} - X_{\text{min}}} \quad (1)$$

For each jam or no jam event, we used the data from 15 days of information before preceding the event was used to predict the event on the 16th day. We generate a balanced dataset with the same number of jam and no-jam events (1008 small sequences totally) was generated, preventing the model from becoming biased to jam or no-jam events. The hydro-meteorological data related to no-jam events were constructed by extracting data from the reaches of no-jam records. To examine models' generalization, we hold out Model generalizations were assessed by extracting 10% of data for testing and 80% and 20% of. With the remaining data, 80% was used for training and 20% for

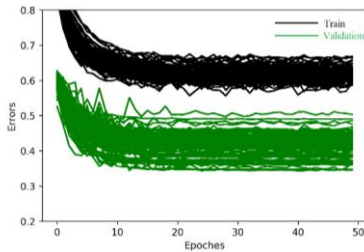
334 validation, ~~respectively~~. We used ShuffleSplit subroutine from the Scikit-learn library, where the database was
335 randomly sampled during each re-shuffling and splitting iteration to generate training and validation sets. We applied
336 100 re-shuffling and splitting iterations for training and validation. There are 726, 181, and 101 small sequences with
337 the size of (16, 7), 16 days of data for the seven variables; for training, validation, and test, respectively.

338 2.6 Training

339 Training a deep neural network with an excellent generalization to new unseen inputs is challenging. As a benchmark,
340 a CNN model with ~~the~~ parameters and layers similar to previous studies (e.g., Ordóñez and Roggen, 2016) is
341 developed. The model shows underfitting or overfitting with various architectures and parameters. To overcome
342 underfitting, deeper models and more nodes ~~in can be added to each layer are beneficial~~; however, overfitting is more
343 challenging to ~~overcome. It is~~ ~~resolve~~. The ice-jam dataset for Quebec contains 1008 balanced sequence instances (with
344 a length of 16), which is ~~small for~~ ~~considered to be a small amount of data in the context of~~ deep learning. ~~The~~
345 ~~deep~~Deep learning models ~~often~~ tend to overfit small datasets by memorizing inputs rather than training, ~~as a~~. ~~This is~~
346 ~~due to the fact that~~ small ~~dataset~~ ~~datasets~~ may not appropriately describe the relationship between input and output
347 spaces.

348 2.6.1 Overcome overfitting

349 There are various ~~methods~~ ~~ways~~ to ~~tackle~~ ~~resolve~~ the problem of overfitting, including acquiring more data, data
350 augmentation (e.g., cropping, rotating, and noise injection), dropout (Srivastava et al., 2014), early stopping, batch
351 normalization (Ioffe and Szegedy, 2015, ~~June~~), and regularization. Acquiring more data is not possible with ice-jam
352 records. We added the Gaussian noise layer (from the Lasagne library), where the noise values are Gaussian-
353 distributed with zero- ~~mean~~ and a standard deviation of 0.1 to the input. The noise layers applied to the CNN and
354 LSTM models significantly overcome the overfitting problem through data augmentation. However, the performance
355 of the CNN-LSTM model dramatically deteriorates, ~~including when~~ a noise layer ~~is added~~ (Fig. 7). Adding a noise
356 layer to other layers does not improve any of the developed models for ice-jam prediction.

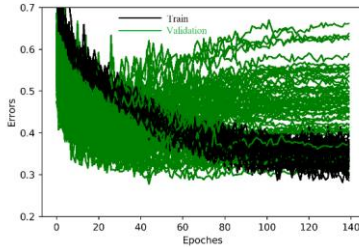


357

358 **Figure 7. Train and validation errors over epochs for CNN-LSTM model with a noise layer.**

359 Early stopping is another efficient method that halts the training procedure ~~at a point~~ where further training would
360 decrease training loss, ~~while~~ ~~but~~ validation loss starts to increase. Neural networks ~~solve~~ ~~need a loss function to~~
361 ~~guide~~ optimization problem ~~that requires a loss function to calculate the model error~~ ~~resolution~~. The loss function is

362 similar to an objective function for process-based hydrological models. Among the developed models, only LSTM
 363 needs early stopping at 40 ~~epoch~~epochs (Fig. 8). More ~~detailed~~ explanations about the ~~other~~ methods that are used in
 364 this study to overcome overfitting (e.g., batch normalization, and L2 regularization) can be found in the Appendix.



365
 366 **Figure_8.** Train and validation errors over epochs for an LSTM model showing overfitting after 40 epochs.

367 **2.6.2 Model ~~Hyperparameters~~hyperparameters**

368 Finding hyperparameter values ~~in deep learning~~ has been challenging due to the complex architecture of deep learning
 369 models and ~~the~~ large number of parameters (Garbin et al., 2020). ~~To find the~~The best model architecture, ~~we study~~
 370 ~~the~~ was identified by assessing model performance ~~of models~~ with different ~~layers~~layer and parameters such as ~~the~~
 371 number of ~~layers~~ (noise, batch normalization, convolutional, pooling, LSTM, dropout, and dense ~~layers~~), as well as
 372 different pooling sizes and strides, different batch sizes, various scaling of data (standardization and normalization),
 373 various filter sizes, number of units in LSTM and dense layers, the type of the activation functions, regularization and
 374 learning rates, weight decay and number of filters in convolutional layers. ~~We also applied various combinations of~~
 375 ~~these layers and parameters.~~Hyperparameters are optimized through manual trial and error
 376 searches as grid search experiments suffer from poor ~~dimensional~~ coverage in dimensions (Bergstra and Bengio, 2012)
 377 ~~and~~). ~~Another reason is that~~ manual experiments are much easier ~~to conduct~~ and ~~more interpretable in~~interpret when
 378 investigating the effect of one hyperparameter of interest. The optimized hyperparameters are presented in Table_3.
 379 The most important parameters of the models are explained below and ~~for more~~additional information ~~about other~~
 380 ~~parameters~~ readers are referred to ~~is~~ available in the Appendix.

381 **Table_3.** Common ~~values~~ and selected values for different parameters of the models.

Parameter	Common values	Selected value	Source
Mini-batch size	16, 32, 64	16	Bengio (2012) ; Devineau et al. (2018b) ; Masters and Luschi (2018)
Number of convolution filters	32, 64, 128	128	Brownlee (2017) ; Maggiori et al. (2017)
Filter size	3, 5, 7	(5,1) and (5,3)	Devineau et al. (2018b) ; Maggiori et al. (2017)
Number of LSTM units	32, 64, 128	128	Brownlee (2017) ; Karim et al. (2019b) ; Ordóñez and Roggen (2016)
Number of dense layer units	16, 32, 128, 256	32	Karim et al. (2019a) ; Livieris et al. (2020) ; Fawaz et al. (2019b)
Momentum in SGD	0.5, 0.99, 0.9	0.9	Brownlee (2018a)

382

Inserted Cells

Formatted Table

Formatted: Left

Formatted: Left

Formatted: Left

Formatted: Left

Formatted: Left

Formatted: Left

Formatted Table

383 **2.6.2.1 Number of layers**

384 The depth of models is related to the sequence length (Devineau et al., 2018, May 2018a), as deeper networks need
385 more data to provide better generalization (Fawaz et al., 2019, July 2019a). In the previous studies offocused on CNNs,
386 there were usually one, two, or three convolution stages (Zheng et al., 2014, June). We tried different numbers of
387 CNN, LSTM, and dense layers and selected the best combination was obtained with three CNN layers, two LSTM
388 layers, and two such dense layers, respectively, as the. The sequence length in this study is small (16), and we could
389 not improve the model performance was not improved by merely adding more simply increasing depth.

390 **2.6.2.2 Number and size of convolution filters**

391 Data with more classes need more filters, and longer time series need longer filters to capture longer patterns and
392 consequently to produce accurate results (Fawaz et al., 2019, July 2019a). However, longer filters significantly increase
393 the number of parameters and potential for overfitting small datasets, while a small filter size risks poor performance.
394 We finally selected In this study, two convolutional layers with 1-D filters of size (5, 1) and stride of (1, 1) to capture
395 temporal variation for each variable separately. Furthermore, one convolutional layer with 2-D filters of size (5, 3)
396 and stride of (1, 1) is then was used to capture the correlation between variables via depth-wise convolution of input
397 time-series. A big stride might cause the model to miss valuable data used in predicting and smoothing out the noise
398 in the time series. The layers in CNNs have a bias for each channel, sharing across all positions in each channel.

399 **2.6.2.4 Adaptive learning rates**

400 The adaptive learning rate decreases the learning rate and consequently weights over each epoch. We tried different
401 base learning and decay rates for each model and found that the learning rate significantly impacts the model's
402 performance. Finally, we chose a base learning rate of 0.1, 0.01, and 0.001 for LSTM, CNN, and CNN-LSTM,
403 respectively. A decay rate of 0.8 was used for CNN and CNN-LSTM, while and a rate of 0.95 for the LSTM model,
404 this rate was 0.95. Table 4 shows the adaptive learning rates for CNN, LSTM, and CNN-LSTM calculated using Eq.
405 (Equation 2) for each epoch.

406
$$\text{adaptive learning rate} = \text{base learning rate} \times \text{decay}^{\text{epoch}} \quad (2)$$

407 The experiments show that the learning rate is the most critical parameter influencing the model performance. A small
408 learning rate can cause the loss function to get stuck in local minima, and a large learning rate can result in oscillations
409 around global minima without reaching it.

410 Our CNN-LSTM model is deeper than the other two models, and deeper models are more prone to a vanishing gradient
411 problem. To overcome the vanishing gradients, it is generally recommended that to use lower learning rates, e.g., lower
412 than $1e-4$, be used. Interestingly, we found that our CNN-LSTM model works better with lower learning rates than
413 the other two models.

414

415 **Table 4. The adaptive learning rate for 50 epochs.**

Learning rate

Epochs	CNN	CNN-LSTM	LSTM
1	0.008	8.00E-04	0.095
2	0.006	6.40E-04	0.09
3	0.005	5.12E-04	0.086
4	0.004	4.10E-04	0.081
.	.	.	.
.	.	.	.
40	1.30E-06	1.33E-07	0.013
.	.	.	.
50	1.40E-07	1.43E-08	-

416

417

418 2.6.5 Model evaluation

419 The network on the validation set is evaluated after each epoch during training to monitor the training progress. During
 420 validation, all non-deterministic layers are switched to deterministic. For instance, noise layers are disabled, and the
 421 update step of the parameters is not performed.

422 The classification accuracy cannot appropriately represent ~~the~~ model performance for unbalanced datasets, as the
 423 model can show a high accuracy by biasing towards the majority class in the dataset (Ordóñez and Roggen, 2016).

424 While we built a balanced dataset (with the same number of jam and no jam events), randomly selecting test data ~~and~~,
 425 shuffling the inputs, and splitting data into train and validation sets can result in a slightly unbalanced dataset. In our
 426 case, the number of jams and no jams for train and validation and test sets is presented in Table-5. Therefore, the F1
 427 score (Eq. (3)), which considers each class equally important, is used to measure the accuracy of binary classification.
 428 The F1 score, as a weighted average of the precision (Eq. (4)) and recall (Eq. (5)), ~~has the best ranges between 0 and~~
 429 ~~worst scores of 1, where 0 is the worse score and 0, respectively, 1 is the best.~~ In ~~Eqs. 7~~equations 4 and 85, TP, FP,
 430 and FN are true positive, false positive, and false negative, respectively.

431 **Table_5. The number of jam and no jam events used in trainthe rain and validation and test datasets.**

	Train and validation	Test
Jam	456	48
No jam	451	53

432
$$F1 = 2 \times \frac{\text{precision} \times \text{recall}}{\text{precision} + \text{recall}} \quad (3)$$

433
$$\text{Precision} = \frac{TP}{TP + FP} \quad (4)$$

434
$$\text{Recall} = \frac{TP}{TP + FN} \quad (5)$$

Formatted: Font: 10 pt

435 Although the model accuracy is usually used to examine the performance of deep learning models, the model size
 436 (i.e., number of parameters) provides a second metric, which represents required memory and calculations, to be
 437 compared among models with the same accuracy (Garbin et al., 2020).

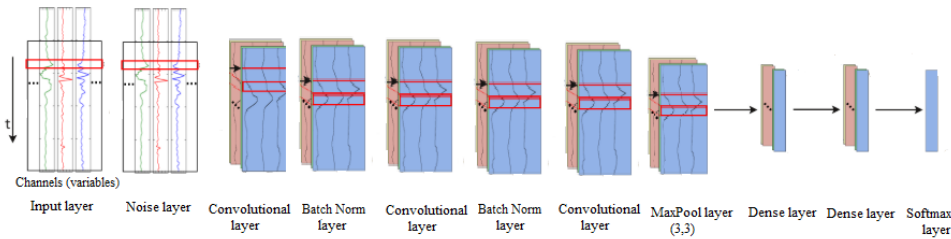
438 After training the model, the well-trained network parameters are saved to a file and are later used for testing the to
 439 test network generalizationgeneralizations using athe test dataset, whichcomposed of data that is not seenused during
 440 training and validation.

441 **2.7 Architecture of models**

442 The architecturesfinal architecture of CNN, LSTM, and CNN-LSTM models that are finally selected are presented in
 443 FigsFigures. 9, 10, and 11, respectively. The layers, their output shapes, and their number of parameters are
 444 respectively presented in Tables- 6, 7, and 8 for CNN, LSTM, and CNN-LSTM models, respectively.

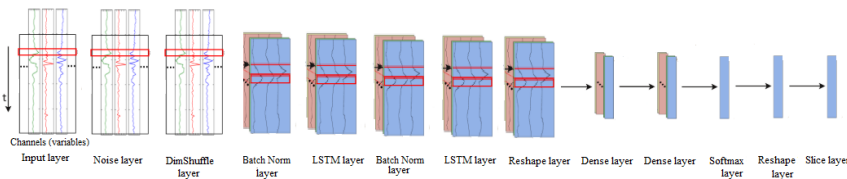
445 The CNNConvolutional NN models often include pooling layers to reduce data complexity and dimensionality.
 446 However, it is not always necessary thatfor every convolutional layer isto be followed by a pooling layer in the time-
 447 series domain (Ordóñez and Roggen, 2016). For instance, Fawaz et al. (2019, July2019a) do not apply any pooling
 448 layers in their TSC_models for TSC. We tried max-pooling layers after different convolutional layers in CNN and
 449 CNN-LSTM networks and found that a pooling layer following only the last convolutional layer improves the
 450 performance of both models. This can be due to subsampling the time series and using time series with a length of 16
 451 that reduceseliminates the need for reducingdecreased dimensionality.

452



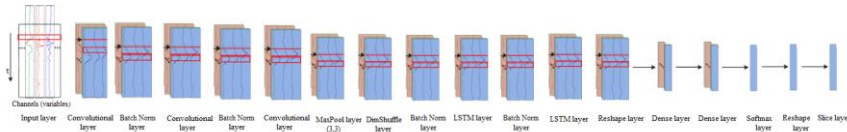
453

454 **Figure-9. The architectureArchitecture** of the CNN model for ice-jam prediction (adapted after Ordóñez and Roggen,
 455 2016).



456

457 **Figure-10. The architectureArchitecture** of the LSTM model for ice-jam prediction (adapted after Ordóñez and Roggen,
 458 2016).



459
460 **Figure-11. The architecture** of the CNN-LSTM model for ice-jam prediction (adapted after Ordóñez and
461 Roggen, 2016).

462 **Table-6. The layers, their Layers, output shapes, and their number of parameters for the CNN model.**

Layers	Output shape	Number of parameters
Input	(16, 1, 16, 7)	0
GaussianNoise	(16, 1, 16, 7)	0
Conv2D	(16, 128, 16, 7)	640
BatchNorm	(16, 128, 16, 7)	512
Nonlinearity	(16, 128, 16, 7)	0
Conv2D	(16, 128, 16, 7)	81920
BatchNorm	(16, 128, 16, 7)	512
Nonlinearity	(16, 128, 16, 7)	0
Conv2D	(16, 128, 16, 7)	245888
MaxPool2D	(16, 128, 5, 2)	0
Dense	(16, 32)	40992
Dense	(16, 32)	1056
Softmax	(16, 2)	66

463
464 **Table-7. The layers, their Layers, output shapes, and their number of parameters for the LSTM model.**

Layers	Output shape	Number of parameters
Input	(16, 1, 16, 7)	0
GaussianNoise	(16, 1, 16, 7)	0
Dimshuffle	(16, 16, 1, 7)	0
BatchNorm	(16, 16, 1, 7)	64
LSTM	(16, 16, 128)	70272
BatchNorm	(16, 16, 128)	64
Nonlinearity	(16, 16, 128)	0
LSTM	(16, 16, 128)	132224
Reshape	(256, 128)	0
Dense	(256, 32)	4128
Dense	(256, 32)	1056
Softmax	(256, 2)	66
Reshape	(16, 16, 2)	0
Slice	(16, 2)	0

465
466 **Table-8. The layers, their Layers, output shapes, and their number of parameters for the CNN-LSTM model.**

Formatted Table

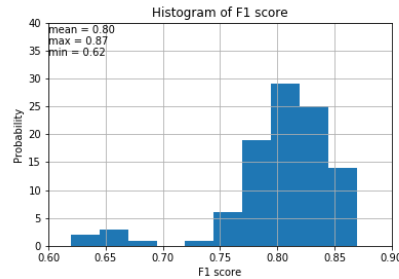
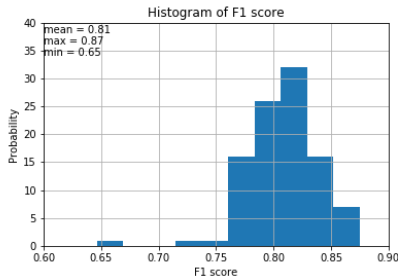
Layers	Output shape	Number of parameters
Input	(16, 1, 16, 7)	0
Conv2D	(16, 128, 16, 7)	640
BatchNorm	(16, 128, 16, 7)	512
Nonlinearity	(16, 128, 16, 7)	0
Conv2D	(16, 128, 16, 7)	81920
BatchNorm	(16, 128, 16, 7)	512
Nonlinearity	(16, 128, 16, 7)	0
Conv2D	(16, 128, 16, 7)	245888
MaxPool2D	(16, 128, 5, 2)	0
Dimshuffle	(16, 5, 128, 2)	0
BatchNorm	(16, 5, 128, 2)	20
LSTM	(16, 5, 128)	197760
BatchNorm	(16, 5, 128)	20
Nonlinearity	(16, 5, 128)	0
LSTM	(16, 5, 128)	132224
Reshape	(80, 128)	0
Dense	(80, 32)	4128
Dense	(80, 32)	1056
Softmax	(80, 2)	66
Reshape	(16, 5, 2)	0
Slice	(16, 2)	0

467

468 3 Results and Discussion

469 3.1 Weight initialization

470 Among ~~all the various types of~~ methods available ~~in Lasagne~~ for weight initialization, ~~in the Lasagne library,~~
471 GLOROT uniform (i.e., Xavier, Glorot and Bengio, 2010, ~~March~~) and He initializations (He et al., 2015); ~~are~~ ~~are~~ the
472 most popular initialization techniques, ~~are used~~ to set the initial random weights in convolutional layers. The results
473 reveal that ~~in our case,~~ these methods yield ~~almost the same comparable~~ F1 scores. However, the histograms of F1
474 scores reveal that GLOROT uniform yields slightly better results (Fig. 12).



475

476 **Figure 12. Histograms of F1 score for CNN using He (left) and GLOROT uniform (right) weight initialization with 100**
 477 **random train-validation splits.**

478 **3.2 Model evaluation**

479 **3.2.1 Learning curves and F1 scores**

480 Line plots of the loss (i.e., learning curves), which are loss over each epoch, are widely used to ~~examine the assess~~
 481 ~~model~~ performance ~~of models~~ in machine learning. Furthermore, line plots clearly indicate common learning
 482 problems, such as underfitting ~~or~~ overfitting. The learning curves for CNN, LSTM, and CNN-LSTM models are
 483 presented in Fig. 13. The LSTM model starts to overfit at epoch 40, so an early stopping is conducted. CNN-LSTM
 484 performs better than the other two models, as its training loss is the lowest and is lower than its validation loss.
 485 Histograms of F1 scores (Fig. 14 and Table 9) show that CNN-LSTM outperforms the other two models since it results
 486 in the highest average and the highest minimum F1-scores for validation (0.82 and 0.75, respectively). Figure 13
 487 shows that the training error of ~~the CNN model~~ is lower than that of ~~the LSTM, which means model, indicating that~~
 488 ~~CNN~~ trained ~~better than LSTM model more efficiently~~. However, it is not true for the validation error. The ~~reason~~
 489 ~~that the validation error is less than the training error in the LSTM model can be the employment because of the~~
 490 regularization methods ~~as used~~. As LSTM models are often harder to regularize, agreeing with previous studies
 491 (e.g., Devineau et al., 2018, June 2018b).

492 The LSTM network is validated better than the CNN model since its average and minimum F1 scores for validation
 493 are better than the CNN model (by 1% and 32%, respectively), and also LSTM yielded no F1 scores below 0.74 (Fig.
 494 14 and Table 9).

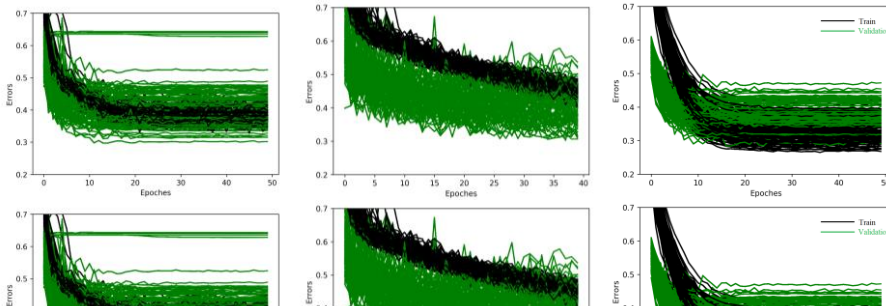
495 As shown in ~~Fig-Figure~~ 13, training loss is higher than validation loss in some of the results. There are some reasons
 496 explaining that. Regularization reduces the validation loss at the expense of increasing training loss. ~~The~~
 497 ~~regularization~~Regularization techniques such as ~~the application of~~ noise layers are only ~~applied used~~
 498 but not during validation resulting in ~~more smooths smoother~~ and usually better functions in validation. There is no
 499 noise layer in CNN-LSTM model that ~~may cause could result in~~ a lower training error than ~~the~~ validation error.
 500 However, other regularization methods such as L2 regularization are used in all the models, including the CNN-LSTM
 501 model.

502 Furthermore, ~~the other issue is that~~ batch normalization uses the mean and variance of each batch ~~induring the~~ training
 503 ~~phase~~, whereas, ~~in validation~~, it uses the mean and variance of the whole training dataset. ~~Plus in the validation phase~~.

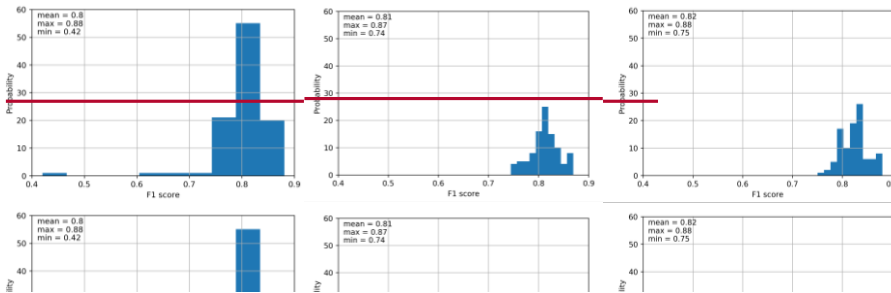
504 Additionally, training loss is averaged over each epoch, while validation losses are calculated after upon completion
505 of each epoch once the current training epoch is completed. Hence, the training loss includes error calculations with
506 fewer updates.

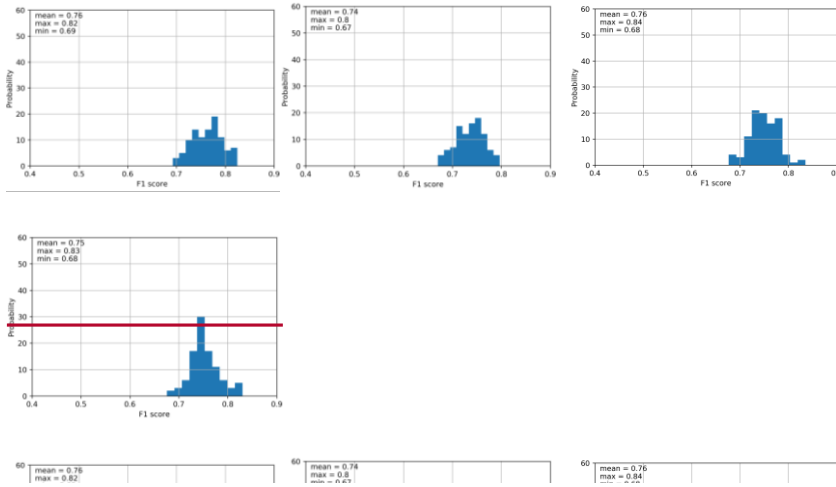
507 Among the developed machine learning models, SVM shows the best validation performance (Figure_15 and
508 Table_10). However, F1 scores of deep learning models are much higher than those of machine learning models with
509 an average of 6% higher F1 score resulted from CNN-LSTM model compared to the SVM model (Tables 9 and 10).

510



511





512

513 **Table-9. F1 scores of the validation phase for CNN, LSTM, and CNN-LSTM models with 100 random train-validation**
 514 **splits.**

<u>Models/Model</u>	<u>F1 score</u>		
	mean	max	min
<u>CNN</u>	0.80	0.88	0.42
<u>LSTM</u>	0.81	0.87	0.74
<u>CNN-LSTM</u>	0.82	0.88	0.75

515

516 **Table-10. F1 scores of the validation phase for SVM, DT, and KNN and MLP models with 100 random train-validation**
 517 **splits.**

<u>Models/Model</u>	<u>F1 score</u>		
	mean	max	min
<u>SVM</u>	0.76	0.82	0.69
<u>DT</u>	0.74	0.80	0.67
<u>KNN</u>	0.75	0.84	0.68
<u>MLP</u>	0.75	0.83	0.68

518 **3.2.2 Number of parameters and run time**

519 The total number of parameters in CNN, LSTM, and CNN-LSTM networks are 371586, 207874, and 664746,
 520 respectively. The CNN-LSTM model had the best performance ~~has resulted from CNN-LSTM~~ with the highest
 521 number of parameters. Even though the number of parameters for the LSTM model is less than that of the CNN model,
 522 the LSTM model shows better validation performance. Furthermore, the number of parameters in the CNN-LSTM
 523 model is much higher than the two other two models, ~~but the without a large increase in computation time is not much~~

Formatted: Font: Times New Roman, 10 pt

Formatted: Left

Formatted Table

Formatted: Font: Times New Roman, 10 pt

Formatted: Centered

Formatted: Font: Times New Roman, 10 pt

Formatted: Font: Times New Roman, 10 pt

Formatted: Font: Times New Roman, 10 pt

Formatted: Font: Times New Roman, 10 pt

Formatted: Font: Times New Roman

Formatted: Font: Times New Roman

Formatted: Font: Times New Roman

Formatted Table

Formatted: Font: Times New Roman

Formatted: Font: Times New Roman

Formatted: Font: Times New Roman

524 ~~higher.~~ All three models ~~take less than were trained within~~ 24 hours ~~to train with using~~ 100 shuffle splits for training
525 and validation. The models ~~are were~~ run on a CPU with four cores, 3.4 GHz clock speed, and 12-GB RAM. ~~On the~~
526 ~~other hand, a few minutes were enough to train the machine learning models with 100 shuffle splits for training and~~
527 ~~validation. Although the training time for deep learning models is much higher than that of machine learning models,~~
528 ~~their superior performance, in this case, justifies their application.~~

529 ~~For all the machine learning models, it took a couple of minutes to train with 100 shuffle splits for training and~~
530 ~~validation. Although, the training time for deep learning models is much higher than that of machine learning models,~~
531 ~~the much better performance of deep learning models justifies their application in our cases.~~

532 3.3 Order of input variables

533 It is not clear ~~that~~ whether the order of input variables in the input file ~~might influencee~~ influences multivariate TSC or
534 not when using 2-D filters and 2-D max-pooling layers. In the benchmark, ~~we randomly used this order model, the~~
535 ~~variables were entered~~ from left to right ~~in the following random order~~: precipitation, minimum temperature,
536 maximum temperature, net radiation, ATDD, AFDD, and snow depth. ~~We randomly changed this order and applied~~
537 ~~the new~~ Another run was conducted by changing the order of the variables for the following random order: snow depth,
538 maximum temperature, precipitation, AFDD, net radiation, minimum temperature, and ATDD. Both models yielded
539 the same average mean and minimum F1 scores, whereas the maximum F1 score ~~from the order in of~~ the benchmark
540 model (0.88) is higher (0.88) than that of the ~~second-order comparative run~~ (0.86). Therefore, it can be concluded that
541 the order does not significantly impact the results.

542 3.4 Testing

543 To examine the ability of the models to generalize to new unseen data, we randomly set aside 10% of the data from
544 the training and validation ~~for phase of~~ all the developed deep learning and machine learning models. ~~We trained a A~~
545 CNN, an LSTM, and a CNN-LSTM model, ~~then the were~~ trained parameters are saved, and ~~finally,~~ the well-trained
546 parameters ~~are utilized for testing. We trained an were saved and used to assess the model's ability to generalize. An~~
547 SVM, a DT, a KNN, and an MLP model ~~and the were also trained. The trained~~ models ~~are were~~ saved and ~~later~~ used
548 for testing. The test dataset is ~~almost an early~~ balanced dataset with 101 samples with the size of (16, 7), including 48
549 jams jam events and 53 ~~no jams-jam events~~.

550 The results of the test models show that the CNN-LSTM model ~~represent had~~ the best F1 score of 0.92 (Table 11).
551 Tables 9 and 11 show that although LSTM ~~has had a~~ slightly ~~better superior~~ validation performance, CNN and LSTM
552 models performed the same in testing.

553 The Testing results of machine learning models ~~for testing are~~ presented in Table 12 ~~indicate that among 11. Among~~
554 the machine learning models, KNN yields the best results with F1 scores of 78%. ~~Tables 11 and 12 declare that deep~~
555 ~~learning models work much better than machine learning models for testing with 14% By comparing CNN LSTM~~
556 ~~with KNN as the best deep learning and machine learning models, model (CNN-LSTM) with the best machine learning~~
557 ~~model (KNN), it can be calculated that the deep learning model outperforms the machine learning model by a~~
558 ~~difference of 14% (F1 score of 92% and 78%, respectively).~~

559

560 Table 11. Test F1 scores for ~~LSTM, CNN, the developed deep learning and CNN-LSTM~~ machine learning models.

Models	F1 score
CNN- LSTM	0.92
CNN	0.80
LSTM	0.80
CNN- LSTMKNN	0.9278

561

562

563

Table 12. Test F1 scores for SVM, DT, and KNN and MLP models.

Models	F1 score
SVM	0.75
DT	0.71
KNN	0.78
MLP	0.70

564

565

3.5 Model comparison

566

567

568

569

570

571

572

573

574

575

576

577

578

579

580

581

582

583

584

585

Multiple Classifiers can be combined classifiers can be considered for and used in pattern recognition problems to reduce errors as different classifiers can cover by covering for one another's internal weaknesses of each other (Parvin et al., 2011). The combined classifier Combined classifiers may be less accurate than the most accurate classifier. However, however, the accuracy of the combined model is always higher than superior to the average accuracy of individual models. Combining two models improved our results compared to convolution-only or LSTM-only networks in both training and testing, supporting the previous studies (e.g., Sainath et al., 2015). It can be because the CNN-LSTM model incorporates both the temporal dependency of each variable by using LSTM networks and the correlation between variables through CNN models. The combined CNN-LSTM model efficiently benefit from automatic feature learning by CNN plus the native support for time series by LSTM.

Although LSTM performed slightly better than outperformed CNN in the validation phase, these models showed the same had comparable performance in the testing phase. The CNN is able to partially include both temporal dependency and the correlation between variables by using 1D-1 and 2D-2 filters, respectively. Although the LSTM is unable to incorporate the correlations between variables, it gives promising results with relatively small dataset and. Another difference is that LSTM captures longer temporal dynamics, while the CNN only captures temporal dynamics comprised within the length of its filters.

Even though our training data in supervised ice-jam prediction is small, the results reveal that deep learning techniques can give accurate results, which agrees with a previous study conducted by Ordóñez and Roggen (2016) in activity recognition. The excellent performance of CNN and CNN-LSTM models may be partially due to the characteristic of CNN that decreases the total number of parameters which does training with limited training data easier (Gao et al., 2016, May). However, we expect our models will be improved in the future by a larger dataset.

Formatted: Font: Times New Roman, 10 pt

Formatted: Font: Times New Roman, 10 pt

Formatted Table

Formatted: Font: Times New Roman, 10 pt

Formatted: Font: Times New Roman, 10 pt

Formatted: Font: Times New Roman, 10 pt, Font color: Auto

Formatted: Font: Times New Roman, 10 pt

Formatted: Font: Times New Roman, 10 pt

Formatted Table

Formatted: Font: 10 pt

Formatted: Font: 10 pt, Font color: Black

Formatted: Font: Times New Roman, 10 pt

Formatted: Font: 10 pt

Formatted: Font: 10 pt, Font color: Black

Formatted: Font: Times New Roman, 10 pt

Formatted Table

Formatted: Font: 10 pt

Formatted: Font: 10 pt, Font color: Black

586 Among the developed machine learning models, SVM showed the best performance in validation, whereas KNN
587 worked the best in testing. However, the performance of deep learning models is much better than machine learning
588 models in both validation and testing. The machine learning models do not consider correlations between variables.
589 However, it is not the only reason that deep learning models worked better than machine learning models. As the
590 LSTM also does not consider correlations between variables but worked better than machine learning models. ~~Some~~
591 ~~characteristics~~This indicates that there are other aspects of ~~developed~~ deep learning models ~~can explain that contribute~~
592 ~~to their~~ ~~better~~high performance ~~compared to machine learning models~~level. For instance, deep learning models
593 perform well for the problems with complex-nonlinear dependencies, time dependencies, and multivariate inputs.
594 The developed CNN-LSTM model can be used for future predictions of ice jams in Quebec to provide early warning
595 of possible floods in the area by using historic hydro-meteorological variables and their predictions for some days in
596 advance.

597 3.6 Discussion on the interpretability of deep learning models

598 Even though the developed deep learning models performed ~~pretty~~well in predicting ice jams in Quebec, the
599 interpretability of the results with respect to the physical processes ~~of the~~involved in ice ~~jam~~jams is still essential. It
600 is because although deep learning models have achieved superior performance in various tasks, these ~~really~~
601 complicated models ~~with~~use a large number of parameters ~~and~~ might ~~sometimes~~ exhibit unexpected behaviours
602 (Samek et al., 2017-~~&~~; Zhang et al., 2021). This is because the real-world environment is still much more complex
603 ~~than any model~~. Furthermore, the models may learn some spurious correlations in the data and make correct
604 predictions ~~with~~for the ~~‘wrong’~~“wrong” reason (Samek and Müller, 2019). Hence, interpretability is especially
605 important in some real-world applications like flood and ice-jam predictions where an error ~~may cause~~could have
606 catastrophic ~~results~~. ~~Also~~consequences. ~~Nonetheless~~, interpretability can be used to extract novel domain knowledge
607 and hidden laws of nature in the research fields with limited domain knowledge (Alipanahi et al., 2015) like ice-jam
608 prediction.

609 However, the nested ~~non-linear~~nonlinear structure and the “black box” nature of deep neural networks make
610 ~~interpretability~~the interpretation of their underlying mechanisms and ~~their~~decisions a significant challenge (Montavon
611 et al., 2018;~~;~~ Zhang et al., 2021-~~and~~; Wojtas and Chen, 2020). That is why, ~~interpretability of~~ deep neural
612 ~~networks~~network interpretability still remains a young and emerging field of research. Nevertheless, there are various
613 methods available to facilitate ~~the~~ understanding of decisions made by a deep learning model such as feature
614 importance ranking, sensitivity analysis, layer-wise relevance propagation, and the global surrogate model. However,
615 the interpretability of developed deep learning models for ice-jam prediction is beyond the scope of this study and it
616 will be investigated in our future works.

617

618 3.7 Model transferability

619 The transferability of a model between river basins is highly desirable but has not yet been achieved because most
620 river ice-jam models are site specific (Mahabir et al., 2007). The developed models in this study can be used to predict
621 future ice jams some days before the event not only for Quebec but ~~can~~ also ~~for~~be transferred to eastern parts of

622 Ontario and western New Brunswick, ~~since these areas have the similar hydro-meteorological conditions~~. For other
623 locations, the developed models ~~can~~ could be ~~transferred via re-training and retrained with~~ a small amount of fine-
624 tuning using ~~labeled~~ labelled instances, rather than building from scratch. ~~If This interesting feature is because due to~~
625 the logic ~~in~~ behind the model ~~may, which could be transferable~~ transferred to the other sites with small modifications.
626 To transfer a model from one river basin to another, ~~historie~~ historical records of ice jams and equivalent hydro-
627 meteorological variables (e.g., precipitation, temperature, and snow depth) ~~as inputs to the model~~ must be available
628 ~~at~~ as model inputs for each site.

629

630 **4 Conclusion**

631 The main finding from this project is that ~~all~~ the developed deep models ~~performed pretty well~~ successfully predicted
632 ~~ice jams in Quebec~~, and performed much better than the developed machine learning models ~~for ice jam prediction in~~
633 ~~Quebec. The comparison of~~. The results show that the CNN-LSTM model is superior to the CNN-only and LSTM-
634 only networks in both validation and testing ~~accuracy, though~~ phases, ~~although~~ the LSTM and CNN ~~models~~
635 ~~demonstrate quite good performance~~ performed well.

636 To our best knowledge, this study is the first ~~study introducing these to apply~~ deep learning models to the ~~problem of~~
637 ice-jam prediction. The developed models are promising ~~to be used to predict future~~ tools for the prediction of ice jams
638 in Quebec and ~~in~~ other ~~similar~~ river basins in Canada with re-training and a small amount of fine-tuning.

639 The developed models do not apply to freeze-up jams that occur in early winter and are based on different processes
640 than breakup jams. We studied only breakup ice jams as usually they result in flooding and are more dangerous than
641 freeze-up jams. Furthermore, there is a lack of data availability for freeze-up ice jams in Quebec and only 89 records
642 of freeze-up jams are available which is too small.

643 The main limitation of this study is ~~data~~ the availability ~~as recorded of ice jams are jam records. Indeed, small which~~
644 ~~causes datasets may lead~~ deep learning models to ~~easily~~ overfit to ~~small number of the~~ data. Another limitation of the
645 presented work is the lack of interpretability of the results with respect to the physical characteristics of the ice jam.
646 This is a topic of future research and our next step is to explore that.

647 ~~The~~ It should also be noted that hydro-meteorological variables are not the only drivers of ice-jam formation. ~~The~~
648 ~~geomorphological indicators that control the formation of ice jams include the~~ Geomorphological features such as
649 river slope, sinuosity, ~~a barrier~~ physical barriers (such as an island or a bridge-), ~~channel~~ narrowing ~~of the channel,~~
650 and ~~river~~ confluence ~~of rivers~~ also govern the formation of ice jams. In the future, a geospatial model using deep
651 learning will be developed to examine the impacts of these geospatial parameters on ice-jam formation.

652 **Author contribution**

653 Fatemehalsadat Madaeni designed and carried out the experiments under Karem Chokmani and Saeid Homayouni
654 supervision. Fatemehalsadat Madaeni developed the model code and performed the simulations using hydro-
655 meteorological and ice-jam data provided and validated by Rachid Lhissou. Fatemehalsadat Madaeni wrote the bulk
656 of the paper with conceptual edits from Karem Chokmani and Saeid Homayouni. Yves Gauthier and Simon
657 Tolszczuk-Leclerc helped in the refinement of the objectives and the revision of the methodological developments.

658 **Acknowledgment**

659 This study is part of the DAVE project, funded by the Defence Research and Development Canada (DRDC), Canadian
660 Safety and Security Program (CSSP), with partners from Natural Resources Canada (NRCan), and Environment and
661 Climate Change Canada.

662 **References**

663 Alipanahi, B., DeLong, A., Weirauch, M. T., & Frey, B. J. (2015). Predicting the sequence specificities of DNA-and
664 RNA-binding proteins by deep learning. *Nature biotechnology*, 33(8), 831-838.

665 Althoff, D., Rodrigues, L. N., & Bazame, H. C. (2021). Uncertainty quantification for hydrological models based on
666 neural networks: the dropout ensemble. *Stochastic Environmental Research and Risk Assessment*, 35(5), 1051-1067.

667 Analytics, C. (2016). *Anaconda Software Distribution: Version 2-2.4. 0*.

668 Apaydin, H., Feizi, H., Sattari, M. T., Colak, M. S., Shamshirband, S., & Chau, K. W. (2020). Comparative analysis
669 of recurrent neural network architectures for reservoir inflow forecasting. *Water*, 12(5), 1500.

670 Barnes-Svarney, P. L., & Montz, B. E. (1985). An ice jam prediction model as a tool in floodplain management. *Water
671 Resources Research*, 21(2), 256-260.

672 Barzegar, R., Aalami, M. T., & Adamowski, J. (2020). Short-term water quality variable prediction using a hybrid
673 CNN-LSTM deep learning model. *Stochastic Environmental Research and Risk Assessment*, 1-19.

674 Barzegar, R., Aalami, M. T., & Adamowski, J. (2021). Coupling a hybrid CNN-LSTM deep learning model with a
675 Boundary Corrected Maximal Overlap Discrete Wavelet Transform for multiscale Lake water level
676 forecasting. *Journal of Hydrology*, 598, 126196.

677 Beltaos, S. (1993). Numerical computation of river ice jams. *Canadian Journal of Civil Engineering*, 20(1), 88-99.

678 [Bengio, Y. \(2012\). Practical recommendations for gradient-based training of deep architectures. *Neural networks: Tricks of the trade*, 437-478.](#)

680 Bergstra, J., & Bengio, Y. (2012). Random search for hyper-parameter optimization. *Journal of machine learning
681 research*, 13(2).

682 [Bergstra, J., Breuleux, O., Bastien, F., Lamblin, P., Pascanu, R., Desjardins, G., ... & Bengio, Y. \(2010, June\). Theano: A CPU and GPU math compiler in Python. In *Proc. 9th Python in Science Conf \(Vol. 1, pp. 3-10\)*.](#)

684 [Brownlee, J. \(2018\). Brownlee, J. \(2017\). Long short-term memory networks with python: develop sequence prediction models with deep learning. *Machine Learning Mastery*.](#)

686 [Brownlee, J. \(2018a\). Better deep learning: train faster, reduce overfitting, and make better predictions. *Machine Learning Mastery*.](#)

687

Formatted: French (Canada)

688 [Brownlee, J. \(2018b\)](#). Deep learning for time series forecasting: predict the future with MLPs, CNNs and LSTMs in
689 Python. Machine Learning Mastery.

690 Brunel, A., Pasquet, J., PASQUET, J., Rodriguez, N., Comby, F., Fouchez, D., & Chaumont, M. (2019). A CNN
691 adapted to time series for the classification of Supernovae. *Electronic Imaging*, 2019(14), 90-1.

692 Brunello, A., Marzano, E., Montanari, A., & Sciavicco, G. (2019). J48SS: A novel decision tree approach for the
693 handling of sequential and time series data. *Computers*, 8(1), 21.

694 Brunner, G. W. (2002). Hec-ras (river analysis system). ~~In~~ North American Water and Environment Congress &
695 Destructive Water ~~(pp. 3782-3787)~~. ASCE.

696 Carson, R. W., Beltaos, S., Healy, D., & Groeneveld, J. (2003, ~~June~~). Tests of river ice jam models—phase 2.
697 ~~In~~ Proceedings of the 12th Workshop on the Hydraulics of Ice Covered Rivers, Edmonton, Alta ~~(pp. 19-20)~~.

698 Carson, R., Beltaos, S., Groeneveld, J., Healy, D., She, Y., Malenchak, J., ... & Shen, H. T. (2011). Comparative
699 testing of numerical models of river ice jams. *Canadian Journal of Civil Engineering*, 38(6), 669-678.

700 Chen, R., Wang, X., Zhang, W., Zhu, X., Li, A., & Yang, C. (2019). A hybrid CNN-LSTM model for typhoon
701 formation forecasting. *GeoInformatica*, 23(3), 375-396.

702 [Cui, Z., Chen, W., & Chen, Y. \(2016\)](#). Multi-scale convolutional neural networks for time series classification. arXiv
703 preprint arXiv:1603.06995.

704 [De Coste, M., Li, Z., Pupek, D., & Sun, W. \(2021\)](#). A hybrid ensemble modelling framework for the prediction of
705 breakup ice jams on Northern Canadian Rivers. *Cold Regions Science and Technology*, 189, 103302.

706 del Campo, F. A., Neri, M. C. G., Villegas, O. O. V., Sánchez, V. G. C., Domínguez, H. D. J. O., & Jiménez, V. G.
707 (2021). Auto-adaptive multilayer perceptron for univariate time series classification. *Expert Systems with*
708 *Applications*, 181, 115147.

709 Devineau, G., Moutarde, F., Xi, W., & Yang, J. (2018, ~~May~~2018a). Deep learning for hand gesture recognition on
710 skeletal data. ~~In~~ 2018-13th IEEE International Conference on Automatic Face & Gesture Recognition ~~(FG 2018)~~ ~~(pp. 106-113)~~. ~~IEEE~~.

712 Devineau, G., Xi, W., Moutarde, F., & Yang, J. (2018, ~~June~~2018b). Convolutional neural networks for multivariate
713 time series classification using both inter-and intra-channel parallel convolutions. ~~In~~ Reconnaissance des Formes,
714 Image, Apprentissage et Perception ~~(RFIAP'2018)~~.

715 Dieleman, S., Schlüter, J., Raffel, C., Olson, E., Sønderby, S.K., Nouri, D., ... & Degraeve, J. (2015). Lasagne: First
716 release. (Version v0.1). Zenodo. Retrieved from <http://doi.org/10.5281/zenodo.27878>.

Formatted: Font: Not Italic

Formatted: Font: Not Italic

Formatted: French (Canada)

Formatted: Font: Not Italic

Formatted: Font: Not Italic

Formatted: English (Canada)

Formatted: English (Canada)

717 Données Québec: Historique (publique) d'embâcles répertoriés au MSP - Données Québec. Retrieved from
718 <https://www.donneesquebec.ca/recherche/dataset/historique-publique-d-embacles-repertoires-au-msp>. (last
719 access: 15 June 2021).

720 Fawaz, H. I., Forestier, G., Weber, J., Idoumghar, L., & Muller, P. A. (2019, July 2019a). Deep neural network
721 ensembles for time series classification. In 2019 International Joint Conference on Neural Networks (IJCNN) (pp. 1-
722 6). IEEE.

723 Fawaz, H. I., Forestier, G., Weber, J., Idoumghar, L., & Muller, P. A. (2019 2019b). Deep learning for time series
724 classification: a review. Data Mining and Knowledge Discovery, 33(4), 917-963.

725 Fischer, T., & Krauss, C. (2018). Deep learning with long short-term memory networks for financial market
726 predictions. European Journal of Operational Research, 270(2), 654-669.

727 Gao, Y., Hendricks, L. A., Kuchenbecker, K. J., & Darrell, T. (2016, May). Deep learning for tactile understanding
728 from visual and haptic data. In 2016 IEEE International Conference on Robotics and Automation (ICRA) (pp. 536-
729 543). IEEE.

730 Garbin, C., Zhu, X., & Marques, O. (2020). Dropout vs. batch normalization: an empirical study of their impact to
731 deep learning. Multimedia Tools and Applications, 1-39.

732 Glorot, X., & Bengio, Y. (2010, March). Understanding the difficulty of training deep feedforward neural networks.
733 In Proceedings of the thirteenth international conference - Thirteenth International Conference on artificial
734 intelligence Artificial Intelligence and statistics (pp. Statistics, 249-256). JMLR Workshop and Conference
735 Proceedings.

736 Graf, R., Kolarski, T., & Zhu, S. (2022). Predicting Ice Phenomena in a River Using the Artificial Neural Network
737 and Extreme Gradient Boosting. Resources, 11(2), 12.

738 Gu, J., Wang, Z., Kuen, J., Ma, L., Shahroudy, A., Shuai, B., ... & Chen, T. (2018). Recent advances in convolutional
739 neural networks. Pattern Recognition, 77, 354-377.

740 Harris, C. R., Millman, K. J., van der Walt, S. J., Gommers, R., Virtanen, P., Cournapeau, D., ... & Oliphant, T. E.
741 (2020). Array programming with NumPy. Nature, 585(7825), 357-362.

742 Hatami, N., Gavet, Y., & Debayle, J. (2018, April). Classification of time-series images using deep convolutional
743 neural networks. In Tenth International Conference on Machine Vision (ICMV 2017) (Vol. 10696, p. 106960Y).
744 International Society for Optics and Photonics.

745 He, K., Zhang, X., Ren, S., & Sun, J. (2015). Delving deep into rectifiers: Surpassing human-level performance on
746 imagenet classification. In Proceedings of the IEEE international conference International Conference on computer
747 vision (pp. Computer Vision, 1026-1034).

748 Hunter, J. D. (2007). Matplotlib: A 2D graphics environment. IEEE Annals of the History of Computing, 9(03), 90-
749 95.

750 Ioffe, S., & Szegedy, C. (2015, ~~June~~). Batch normalization: Accelerating deep network training by reducing internal
751 covariate shift. In-International conferenceConference on machine learning (pp-Machine Learning, 448-456). PMLR.

752 Jović, A., Brkić, K., & Bogunović, N. (2012, ~~August~~). Decision tree ensembles in biomedical time-series
753 classification. In-Joint DAGM (German Association for Pattern Recognition) and OAGM Symposium (pp-2, 408-417).
754 Springer, Berlin, Heidelberg.

755 Jozefowicz, R., Zaremba, W., & Sutskever, I. (2015, ~~June~~). An empirical exploration of recurrent network
756 architectures. In-International conferenceConference on machine learning (pp-Machine Learning, 2342-2350). PMLR.

757 Karim, F., Majumdar, S., & Darabi, H. (2019a). Insights into LSTM fully convolutional networks for time series
758 classification. IEEE Access, 7, 67718-67725.

759 Karim, F., Majumdar, S., Darabi, H., & Chen, S. (2017). LSTM fully convolutional networks for time series
760 classification. IEEE access, 6, 1662-1669.

761 Karim, F., Majumdar, S., Darabi, H., & Harford, S. (~~2019~~2019b). Multivariate lstm-fcns for time series
762 classification. Neural Networks, 116, 237-245.

763 Kashiparekh, K., Narwariya, J., Malhotra, P., Vig, L., & Shroff, G. (2019, ~~July~~). ConvTimeNet: A pre-trained deep
764 convolutional neural network for time series classification. In-2019-International Joint Conference on Neural
765 Networks (IJCNN) (pp-2, 1-8). IEEE.

766 Kratzert, F., Klotz, D., Brenner, C., Schulz, K., & Herrnegger, M. (2018). Rainfall-runoff modelling using long short-
767 term memory (LSTM) networks. Hydrology and Earth System Sciences, 22(11), 6005-6022.

768 Li, D., Djulovic, A., & Xu, J. F. (2013). A Study of kNN using ICU multivariate time series data. In Proc. Int. Conf.
769 Data Mining, eds. R. Stahlbock and GM Weiss (DMIN, 2013) (pp-2, 211-217).

770 Li, X., Zhang, Y., Zhang, J., Chen, S., Marsic, I., Farneth, R. A., & Burd, R. S. (2017). Concurrent activity recognition
771 with multimodal CNN-LSTM structure. arXiv preprint arXiv:1702.01638.

772 Lin, J., Williamson, S., Borne, K., & DeBarr, D. (2012). Pattern recognition in time series. Advances in Machine
773 Learning and Data Mining for Astronomy, 1, 617-645.

774 Lindenschmidt, K. E. (2017). RIVICE—a non-proprietary, open-source, one-dimensional river-ice
775 model. Water, 9(5), 314.

776 Lipton, Z. C., Berkowitz, J., & Elkan, C. (2015). A critical review of recurrent neural networks for sequence
777 learning. arXiv preprint arXiv:1506.00019.

Formatted: French (Canada)

Formatted: Font: Not Italic

Formatted: Font: Not Italic

778 Livieris, I. E., Pintelas, E., & Pintelas, P. (2020). A CNN-LSTM model for gold price time-series forecasting. *Neural*
779 *computing and applications*, 32(23), 17351-17360.

780 Lu, N., Wu, Y., Feng, L., & Song, J. (2018). Deep learning for fall detection: Three-dimensional CNN combined with
781 LSTM on video kinematic data. *IEEE journal of biomedical and health informatics*, 23(1), 314-323.

782 Luan, Y., & Lin, S. (2019, ~~March~~). Research on text classification based on CNN and LSTM. ~~In 2019 IEEE~~
783 ~~international conference~~International Conference on artificial intelligenceArtificial Intelligence and computer
784 applications (ICAICA) (pp. Computer Applications, 352-355). IEEE.

785 Madaeni, F., Lhissou, R., Chokmani, K., Raymond, S., & Gauthier, Y. (2020). Ice jam formation, breakup and
786 prediction methods based on hydroclimatic data using artificial intelligence: A review. *Cold Regions Science and*
787 *Technology*, 103032.

788 Maggiori, E., Tarabalka, Y., Charpiat, G., & Alliez, P. (2017). High-resolution aerial image labeling with
789 convolutional neural networks. IEEE Transactions on Geoscience and Remote Sensing, 55(12), 7092-7103.

790 Mahabir, C., Hicks, F. E., & Fayek, A. R. (2007). Transferability of a neuro-fuzzy river ice jam flood forecasting
791 model. *Cold Regions Science and Technology*, 48(3), 188-201.

792 Mahabir, C., Hicks, F., & Fayek, A. R. (2006). Neuro-fuzzy river ice breakup forecasting system. *Cold regions science*
793 *and technology*, 46(2), 100-112.

794 Mahfouf, J. F., Brasnett, B., & Gagnon, S. (2007). A Canadian precipitation analysis (CaPA) project: Description and
795 preliminary results. *Atmosphere-ocean*, 45(1), 1-17.

796 Massie, D.D., White, K.D., Daly, S.F., ~~(2002-)~~. Application of neural networks to predict ice jam occurrence. *Cold*
797 ~~Reg. Sci. Technol.~~Regions Science and Technology, 35 (2), 115-122.

798 Masters, D., & Luschi, C. (2018). Revisiting small batch training for deep neural networks. arXiv preprint
799 arXiv:1804.07612.

800 Mesinger, F., DiMego, G., Kalnay, E., Mitchell, K., Shafran, P. C., Ebisuzaki, W., ... & Shi, W. (2006). North
801 American regional reanalysis. *Bulletin of the American Meteorological Society*, 87(3), 343-360.

802 Montavon, G., Samek, W., & Müller, K. R. (2018). Methods for interpreting and understanding deep neural
803 networks. *Digital Signal Processing*, 73, 1-15.

804 Mutegeki, R., & Han, D. S. (2020, ~~February~~). A CNN-LSTM approach to human activity recognition. ~~In 2020~~
805 ~~International Conference on Artificial Intelligence in Information and Communication (ICA3IC) (pp. 362-366). IEEE.~~

806 Nanopoulos, A., Alcock, R., & Manolopoulos, Y. (2001). Feature-based classification of time-series
807 data. *International Journal of Computer Research*, 10(3), 49-61.

808 National Hydro Network - NHN - GeoBase Series - Natural Resources Canada. Retrieved from
809 <https://open.canada.ca/data/en/dataset/a4b190fe-e090-4e6d-881e-b87956c07977>.

810 National Hydrographic Network - Natural Resources Canada. Retrieved from [https://www.nrcan.gc.ca/science-and-
data/science-and-research/earth-sciences/geography/topographic-information/geobase-surface-water-program-
geeau/national-hydrographic-network/21361](https://www.nrcan.gc.ca/science-and-

811 data/science-and-research/earth-sciences/geography/topographic-information/geobase-surface-water-program-

812 geeau/national-hydrographic-network/21361).

813 Nosratabadi, S., Mosavi, A., Duan, P., Ghamisi, P., Filip, F., Band, S. S., ... & Gandomi, A. H. (2020). Data science
814 in economics: comprehensive review of advanced machine learning and deep learning methods. *Mathematics*, 8(10),
815 1799.

816 Oh, S. L., Ng, E. Y., San Tan, R., & Acharya, U. R. (2018). Automated diagnosis of arrhythmia using combination of
817 CNN and LSTM techniques with variable length heart beats. *Computers in biology and medicine*, 102, 278-287.

818 Olah, C. (2015). Understanding LSTM Networks. Retrieved— from [https://colah.github.io/posts/2015-08-
Understanding-LSTMs/](https://colah.github.io/posts/2015-08-

819 Understanding-LSTMs/).

820 Ombabi, A. H., Ouarda, W., & Alimi, A. M. (2020). Deep learning CNN–LSTM framework for Arabic sentiment
821 analysis using textual information shared in social networks. *Social Network Analysis and Mining*, 10(1), 1-13.

822 Ordóñez, F. J., & Roggen, D. (2016). Deep convolutional and lstm recurrent neural networks for multimodal wearable
823 activity recognition. *Sensors*, 16(1), 115.

824 Parvin, H., Minaei, B., Beigi, A., & Helmi, H. (2011, ~~April~~). Classification ensemble by genetic algorithms.
825 ~~In~~-International Conference on Adaptive and Natural Computing Algorithms (pp. 391-399). ~~Springer, Berlin,
826 Heidelberg.~~

827 Pedregosa, F., Varoquaux, G., Gramfort, A., Michel, V., Thirion, B., Grisel, O., ... & Duchesnay, E. (2011). Scikit-
828 learn: Machine learning in Python. ~~the~~The Journal of ~~machine~~Machine Learning ~~research~~Research, 12.

829 Prowse, T. D., & Bonsal, B. R. (2004). Historical trends in river-ice break-up: a review. *Hydrology Research*, 35 (4-
830 5), 281-293.

831 Prowse, T. D., Bonsal, B. R., Duguay, C. R., & Lacroix, M. P. (2007). River-ice break-up/freeze-up: a review of
832 climatic drivers, historical trends and future predictions. *Annals of Glaciology*, 46, 443-451.

833 Raybaut, P. (2009). Spyder-documentation. Retrieved from pythonhosted.org.

834 Reback, J., McKinney, W., Den Van Bossche, J., Augspurger, T., Cloud, P., Klein, A., ... & Seabold, S. (2020).
835 pandas-dev/pandas: Pandas 1.0. 3. Zenodo.

836 Rodríguez, J. J., & Alonso, C. J. (2004, ~~December~~). Support vector machines of interval-based features for time series
837 classification. ~~In~~-International Conference on Innovative Techniques and Applications of Artificial Intelligence (pp.
838 244-257). ~~Springer, London.~~

Formatted: French (Canada)

839 Sainath, T. N., Vinyals, O., Senior, A., & Sak, H. (2015, ~~April~~). Convolutional, long short-term memory, fully
840 connected deep neural networks. ~~In 2015 IEEE International Conference on Acoustics, Speech and Signal Processing~~
841 ~~(ICASSP) (pp. 4580-4584). IEEE.~~

842 Samek, W., & Müller, K. R. (2019). Towards explainable artificial intelligence. ~~In Explainable AI: interpreting,~~
843 ~~explaining Interpreting, Explaining and visualizing deep learning (pp. Visualizing Deep Learning, 5-22). Springer,~~
844 ~~Cham.~~

845 Samek, W., Wiegand, T., & Müller, K. R. (2017). Explainable artificial intelligence: Understanding, visualizing and
846 interpreting deep learning models. arXiv preprint arXiv:1708.08296.

847 [Sarafanov, M., Borisova, Y., Maslyayev, M., Revin, I., Maximov, G., & Nikitin, N. O. \(2021\). Short-Term River Flood](#)
848 [Forecasting Using Composite Models and Automated Machine Learning: The Case Study of Lena](#)
849 [River. Water, 13\(24\), 3482.](#)

850 [Semenova, N., Sazonov, A., Krylenko, I., & Frolova, N. \(2020\). Use of classification algorithms for the ice jams](#)
851 [forecasting problem. E3S Web of Conferences.](#)

852 She, X., & Zhang, D. (2018, ~~December~~). Text classification based on hybrid CNN-LSTM hybrid model. ~~In 2018 11th~~
853 ~~International Symposium on Computational Intelligence and Design (ISCID) (Vol. 2, pp. 185-189). IEEE.~~

854 Shouyu, C., & Honglan, J. (2005). Fuzzy Optimization Neural Network Approach for Ice Forecast in the Inner
855 Mongolia Reach of the Yellow River/Approche d'Optimisation Floue de Réseau de Neurones pour la Prévision de la
856 Glace Dans le Tronçon de Mongolie Intérieure du Fleuve Jaune. Hydrological sciences journal, 50(2).

857 Sosa, P. M. (2017). Twitter sentiment analysis using combined LSTM-CNN models. Eprint Arxiv, 1-9.

858 Srivastava, N., Hinton, G., Krizhevsky, A., Sutskever, I., & Salakhutdinov, R. (2014). Dropout: a simple way to
859 prevent neural networks from overfitting. The journal of machine learning research, 15(1), 1929-1958.

860 The Atlas of Canada - Toporama - Natural Resources Canada. Retrieved from
861 <https://atlas.gc.ca/toporama/en/index.html>.

862 Thornton, M.M., Shrestha, R., Wei, Y., Thornton, P.E., Kao, S. & Wilson, B.E. (2020). Daymet: Daily Surface
863 Weather Data on a 1-km Grid for North America, Version 4. ORNL DAAC, Oak Ridge, Tennessee, USA.

864 Torres, J. F., Hadjout, D., Sebaa, A., Martínez-Álvarez, F., & Troncoso, A. (2021). Deep Learning for Time Series
865 Forecasting: A Survey. Big Data, 9(1), 3-21.

866 Turcotte, B., & Morse, B. (2015, ~~August~~). River ice breakup forecast and annual risk distribution in a climate change
867 perspective. ~~In 18th Workshop on the Hydraulics of Ice Covered Rivers, CGU HS Committee on River Ice Processes~~
868 ~~and the Environment, Quebec (Vol. 35).~~

Formatted: English (Canada)

869 Umer, M., Imtiaz, Z., Ullah, S., Mehmood, A., Choi, G. S., & On, B. W. (2020). Fake news stance detection using
870 deep learning architecture (cnn-lstm). *IEEE Access*, 8, 156695-156706.

871 Wang, J., Yu, L. C., Lai, K. R., & Zhang, X. (2016, ~~August~~). Dimensional sentiment analysis using a regional CNN-
872 LSTM model. ~~In Proceedings of the 54th annual meeting~~Annual Meeting of the ~~association~~Association for
873 ~~computational linguistics (volume 2: Short papers) (pp. Computational Linguistics, 225-230).~~

874 Wang, J., Yu, L. C., Lai, K. R., & Zhang, X. (2019). Tree-structured regional CNN-LSTM model for dimensional
875 sentiment analysis. *IEEE/ACM Transactions on Audio, Speech, and Language Processing*, 28, 581-591.

876 White, K. D. (2003). Review of prediction methods for breakup ice jams. *Canadian Journal of Civil Engineering*,
877 30(1), 89-100.

878 White, K. D., & Daly, S. F. (2002, ~~January~~). Predicting ice jams with discriminant function analysis. ~~In ASME 2002~~
879 ~~21st International Conference on Offshore Mechanics and Arctic Engineering (pp. 683-690).~~ ~~American Society of~~
880 ~~Mechanical Engineers.~~

881 Wojtas, M., & Chen, K. (2020). Feature importance ranking for deep learning. arXiv preprint arXiv:2010.08973.

882 Wu, J., Yao, L., & Liu, B. (2018a, ~~April~~2018). An overview on feature-based classification algorithms for multivariate
883 time series. ~~In 2018 IEEE 3rd International Conference on Cloud Computing and Big Data Analysis (ICCCBDA) (pp.~~
884 ~~32-38).~~ ~~IEEE.~~

885 Wu, Z., Wang, X., Jiang, Y. G., Ye, H., & Xue, X. (2015, ~~October~~). Modeling spatial-temporal clues in a hybrid deep
886 learning framework for video classification. ~~In Proceedings of the 23rd ACM international conference~~International
887 Conference on Multimedia ~~(pp. 461-470).~~

888 Wunsch, A., Liesch, T., & Broda, S. (2020). Groundwater Level Forecasting with Artificial Neural Networks: A
889 Comparison of LSTM, CNN and NARX. *Hydrology and Earth System Sciences Discussions*, 2020, 1-23.

890 Xing, Z., Pei, J., & Keogh, E. (2010). A brief survey on sequence classification. *ACM Sigkdd Explorations*
891 *Newsletter*, 12(1), 40-48.

892 Xingjian, S. H. I., Chen, Z., Wang, H., Yeung, D. Y., Wong, W. K., & Woo, W. C. (2015). Convolutional LSTM
893 network: A machine learning approach for precipitation nowcasting. ~~In Advances in neural information processing~~
894 ~~systems (pp. 802-810).~~

895 Yan, J., Mu, L., Wang, L., Ranjan, R., & Zomaya, A. Y. (2020). Temporal convolutional networks for the advance
896 prediction of ENSO. *Scientific reports*, 10(1), 1-15.

897 Yang, J., Nguyen, M. N., San, P. P., Li, X. L., & Krishnaswamy, S. (2015, ~~June~~). Deep convolutional neural networks
898 on multichannel time series for human activity recognition. ~~In Twenty-fourth international joint~~
899 ~~conference~~International Joint Conference on ~~artificial intelligence~~Artificial Intelligence.

900 Yi, S., Ju, J., Yoon, M. K., & Choi, J. (2017). Grouped convolutional neural networks for multivariate time
901 series. arXiv preprint arXiv:1703.09938.

902 Zhang, D., Lin, J., Peng, Q., Wang, D., Yang, T., Sorooshian, S., ... & Zhuang, J. (2018). Modeling and simulating of
903 reservoir operation using the artificial neural network, support vector regression, deep learning algorithm. *Journal of*
904 *Hydrology*, 565, 720-736.

905 Zhang, Y., Tiño, P., Leonardis, A., & Tang, K. (2021). A survey on neural network interpretability. *IEEE Transactions*
906 *on Emerging Topics in Computational Intelligence*.

907 Zhao, L., Hicks, F. E., & Fayek, A. R. (2012). Applicability of multilayer feed-forward neural networks to model the
908 onset of river breakup. *Cold Regions Science and Technology*, 70, 32-42.

909 Zheng, Y., Liu, Q., Chen, E., Ge, Y., & Zhao, J. L. (2014, ~~June~~). Time series classification using multi-channels deep
910 convolutional neural networks. ~~In-International Conference on Web-Age Information Management (pp. 298-310).~~
911 ~~Springer, Cham.~~

912 Zheng, Y., Liu, Q., Chen, E., Ge, Y., & Zhao, J. L. (2016). Exploiting multi-channels deep convolutional neural
913 networks for multivariate time series classification. *Frontiers of Computer Science*, 10(1), 96-112.

914

915